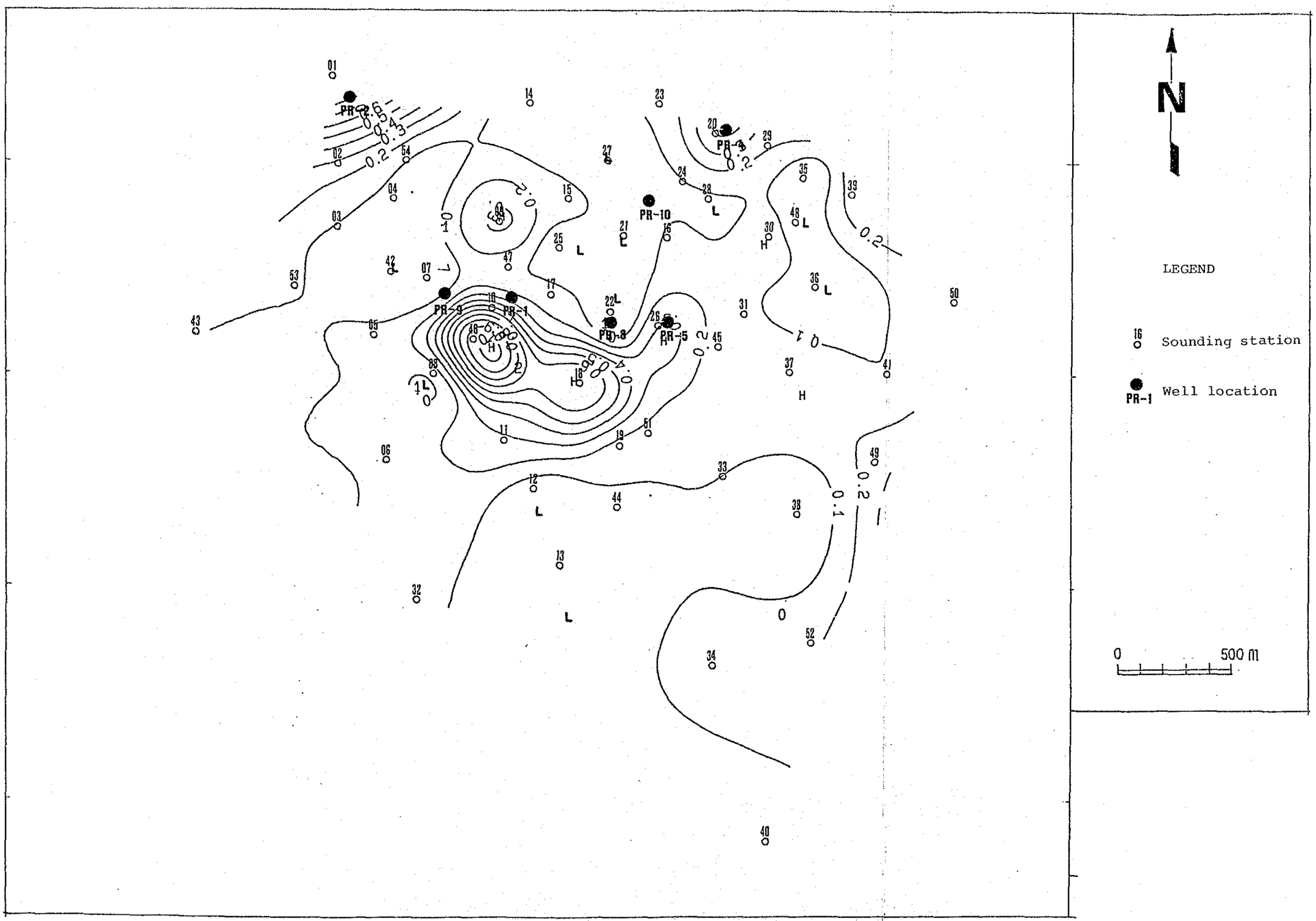

Fig. 29. Distribution map of Tipper magnitude, period = 30 sec.

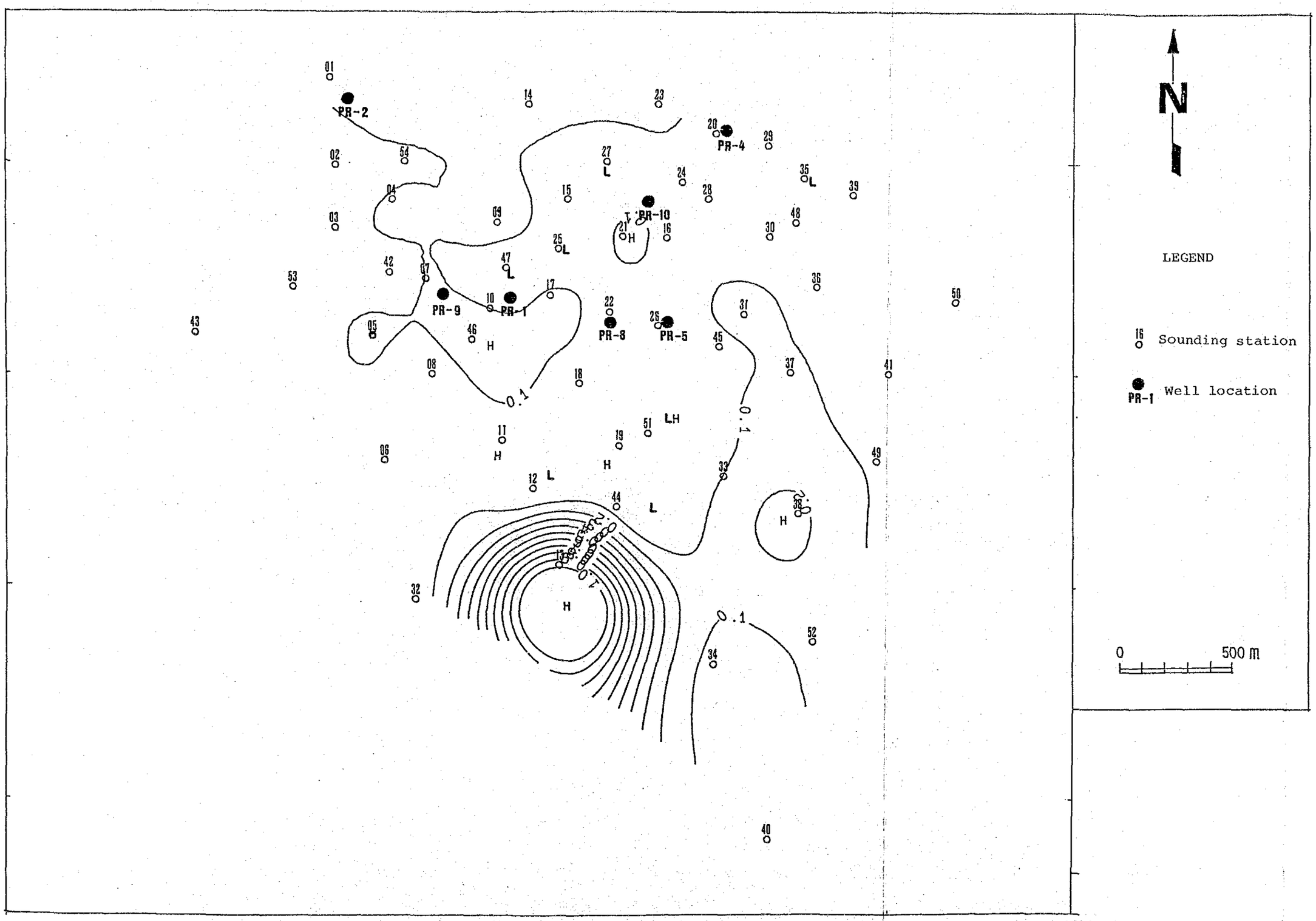

Fig. 30. Distribution map of Skew, period = 30 sec.

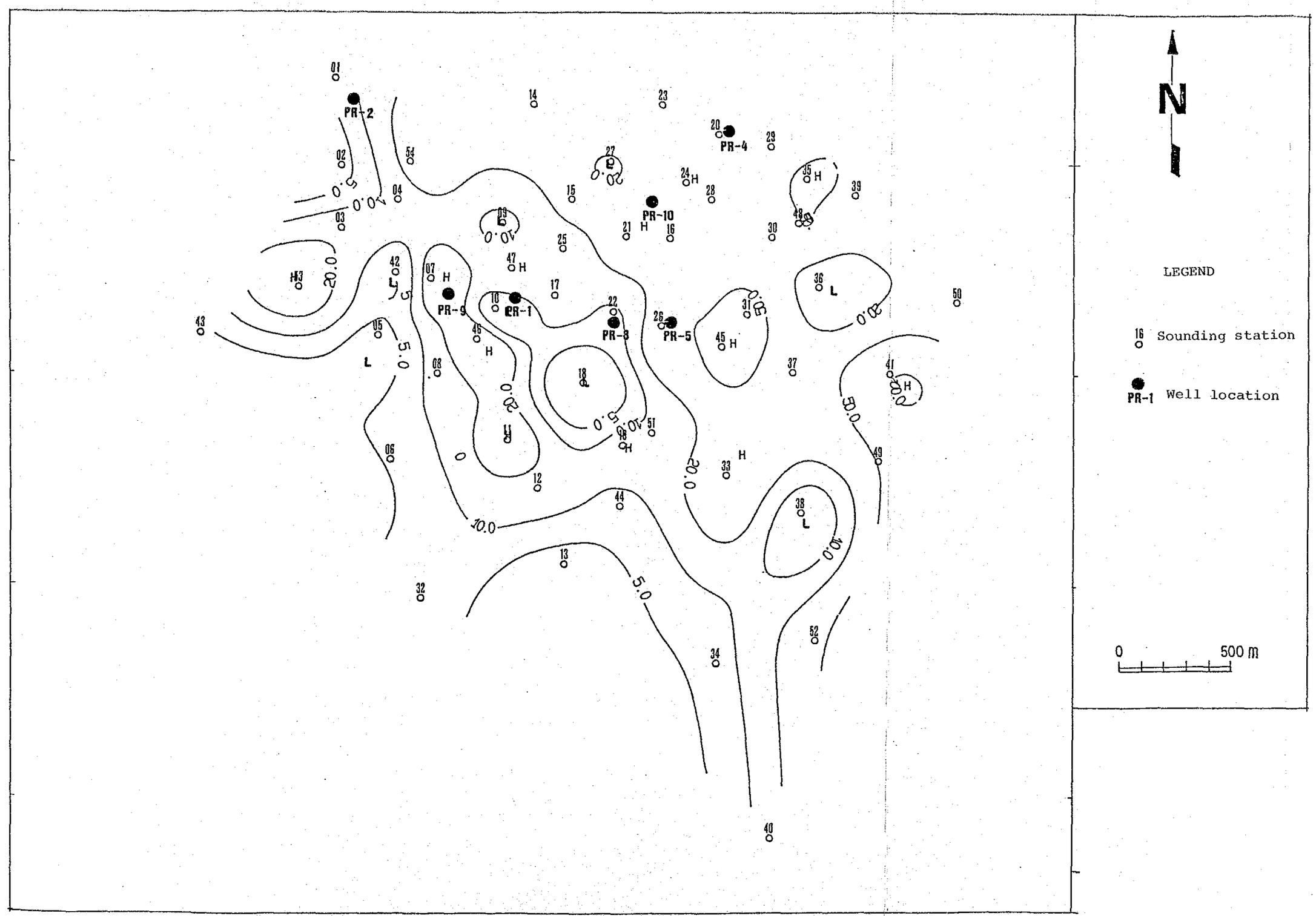

Fig. 31. Apparent resistivity map (TE mode), period = 30 sec.

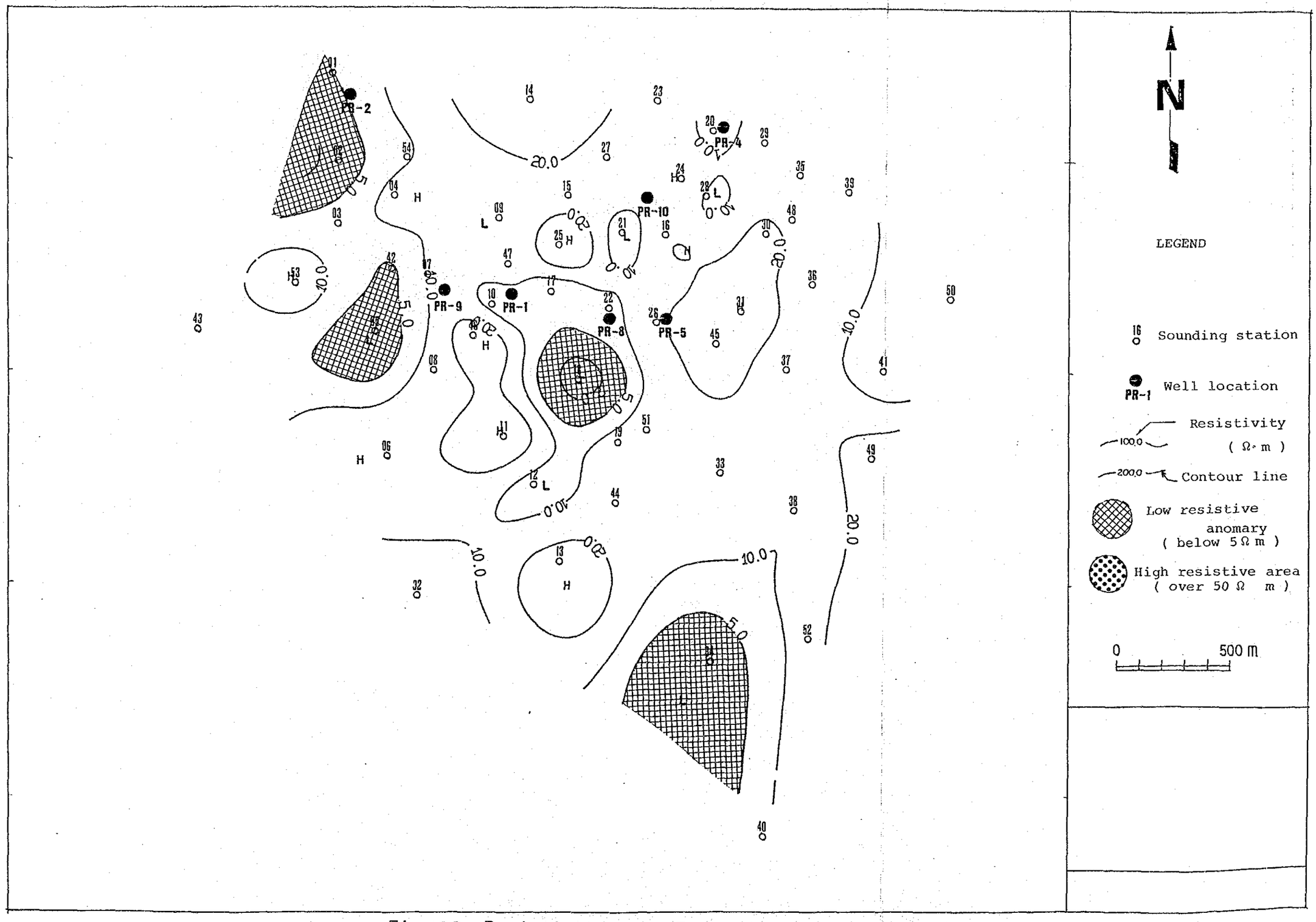

Fig. 32. Resistivity map (TE mode), Om above sea level

Fig. 33. Resistivity map (TE mode), 500m below sea level

PSEUD CROSS SECTION

Area
PRIMAVERA

MODE
TE

No.
3

Resistivity
(Ω.m)

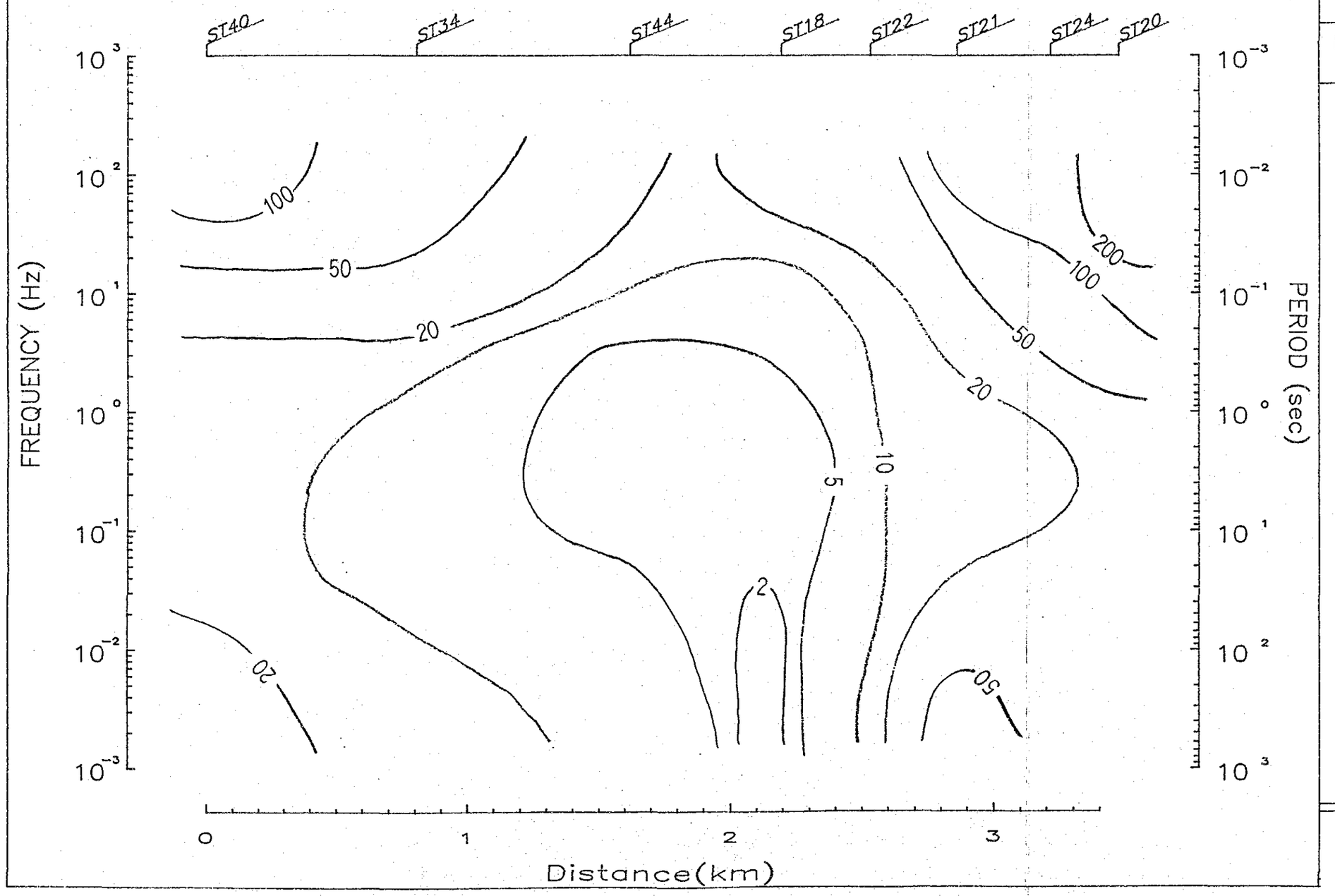

Fig. 34. Apparent resistivity pseudo-cross section (TE mode), line 3

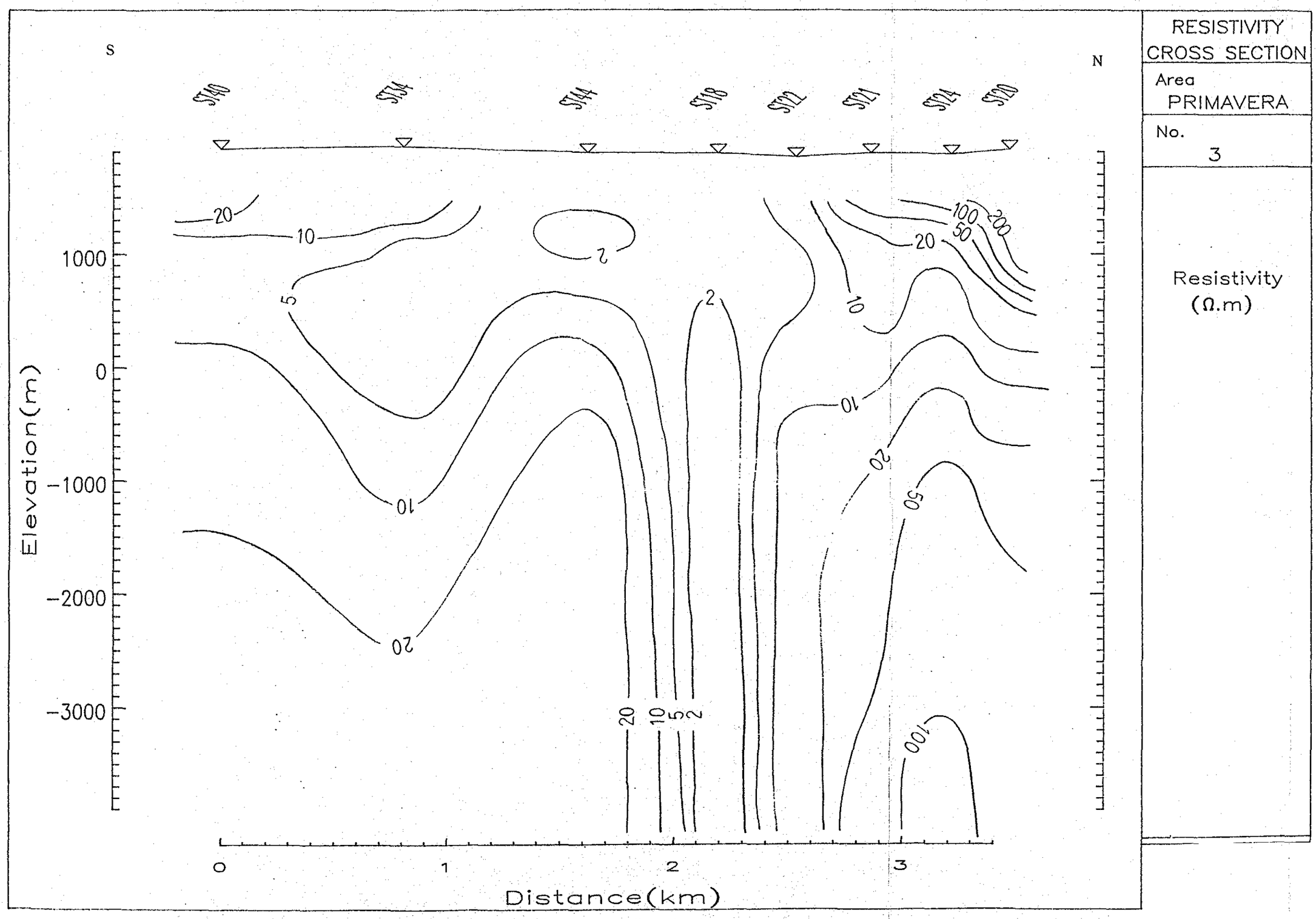

Fig. 35. Resistivity cross section (TE mode), line 3.

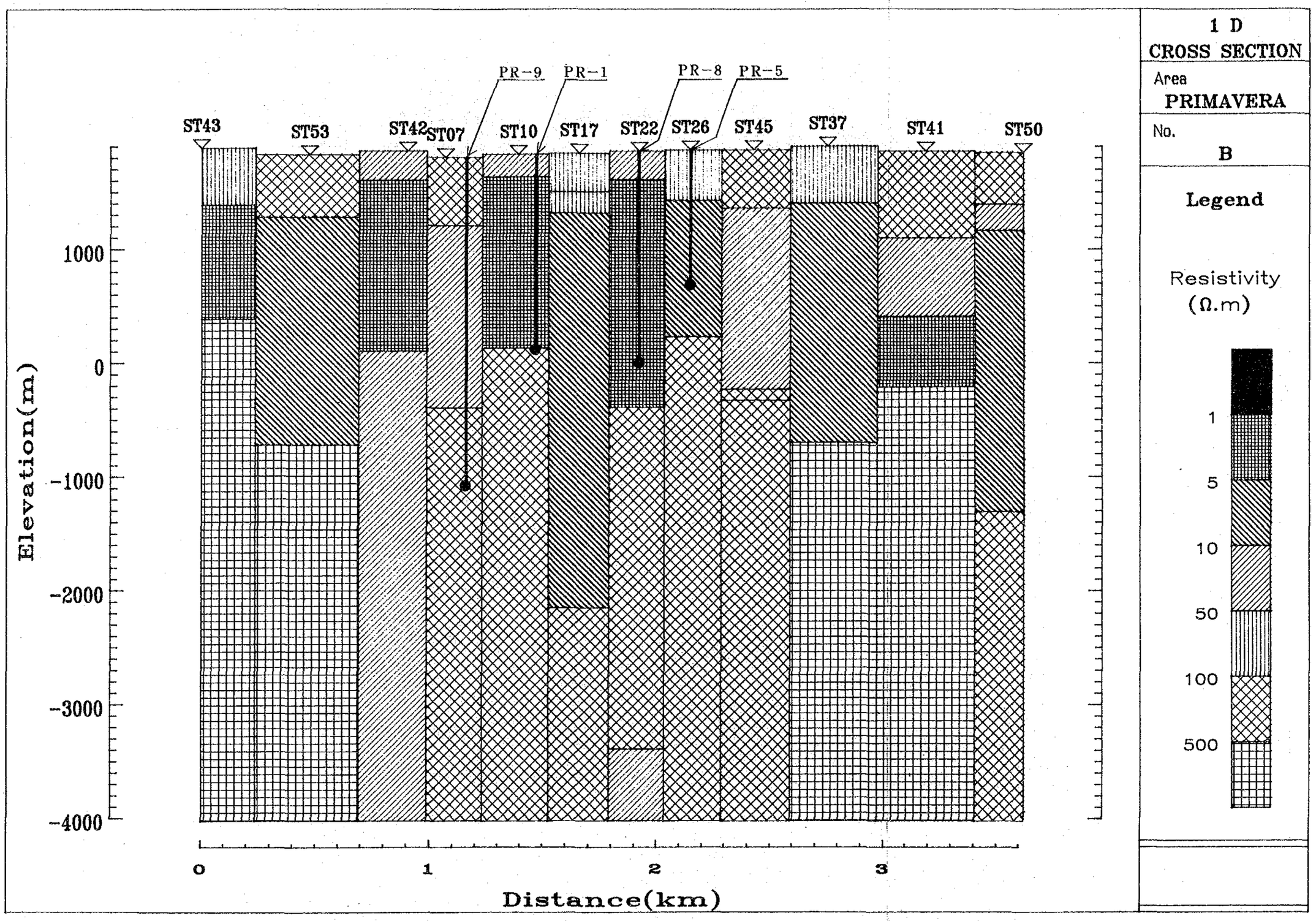

Fig. 36. 1-D model cross section line B.

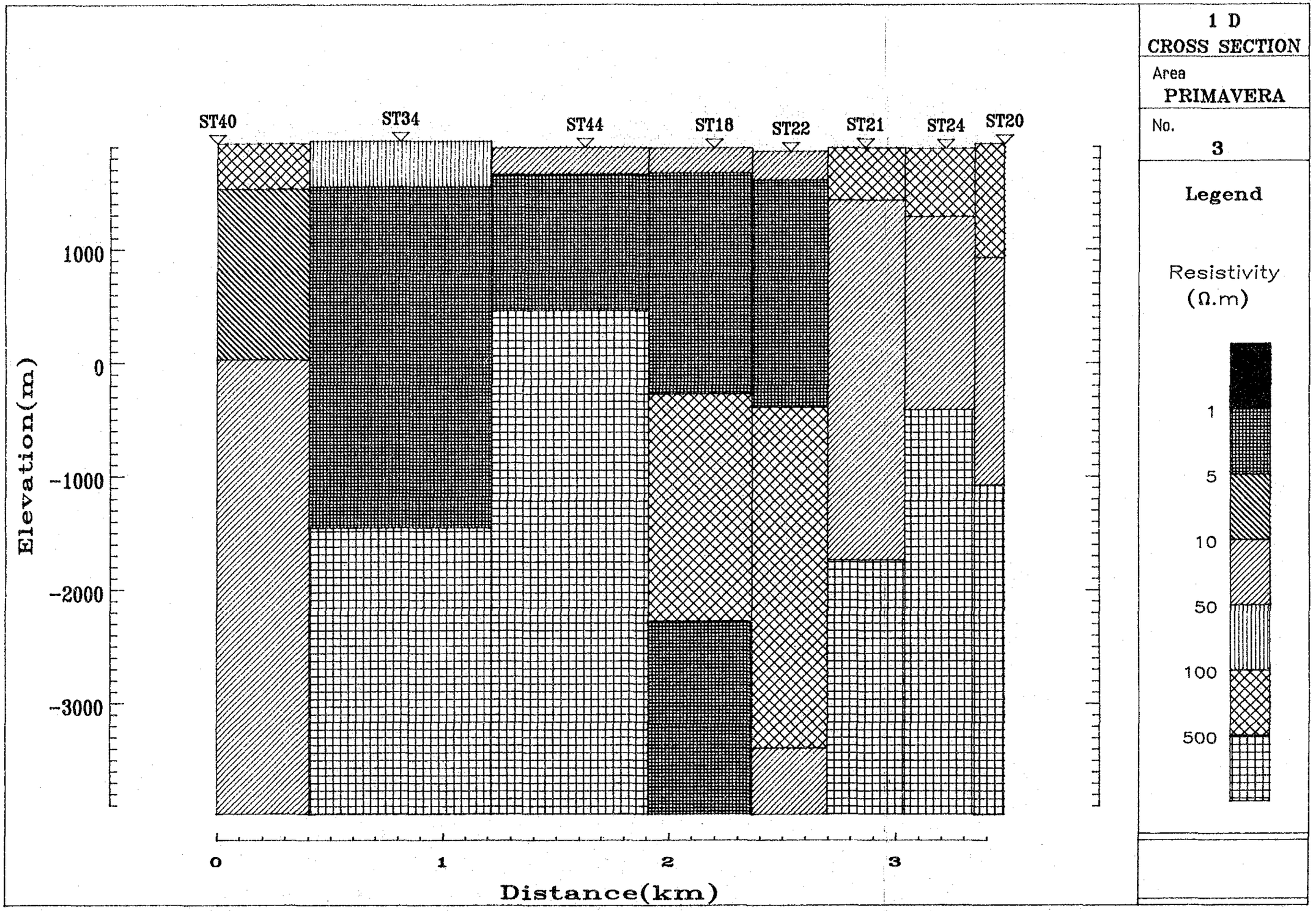

Fig. 37. 1-D model cross section line 3.

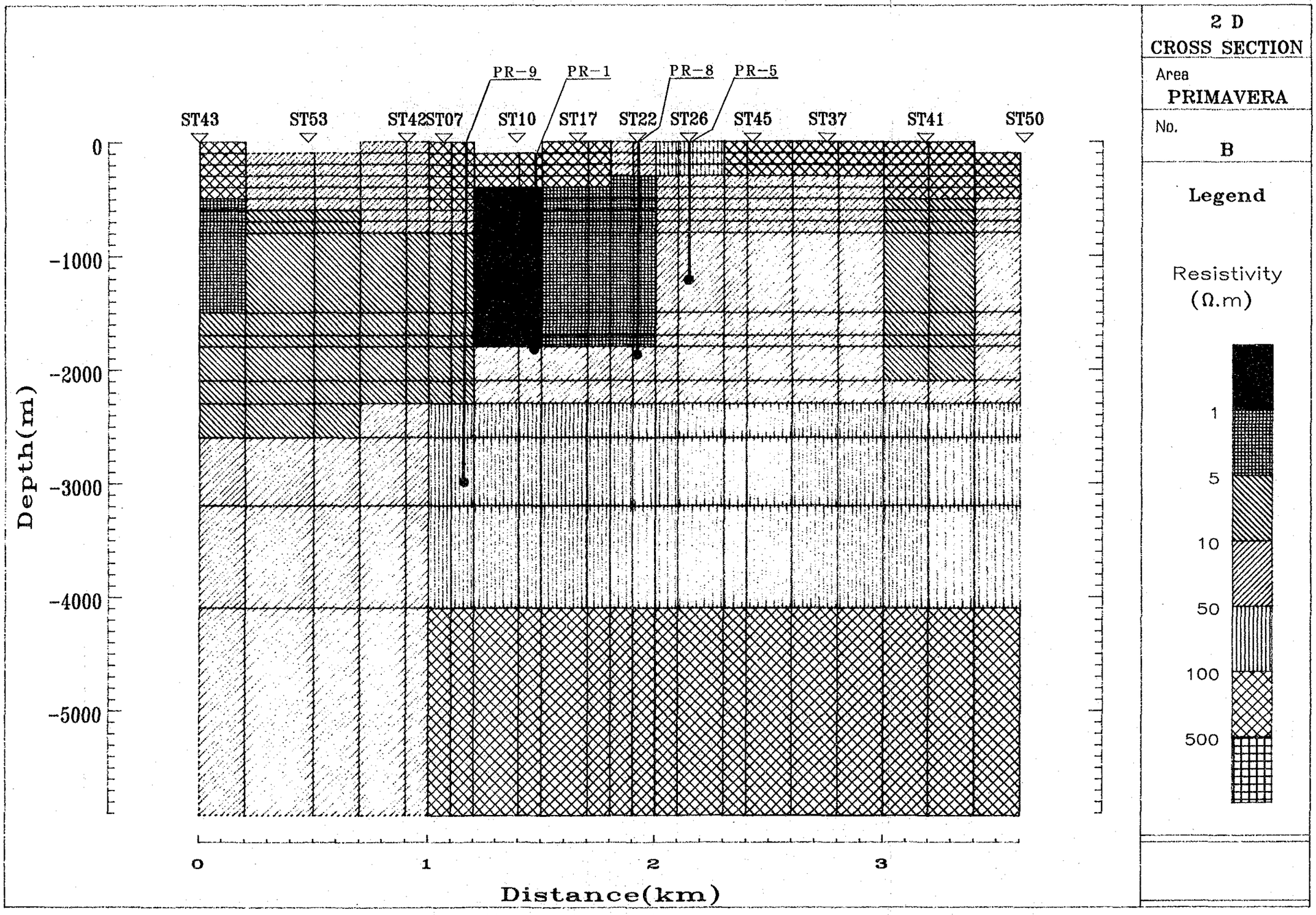

Fig. 38. 2-D model cross section, line B.

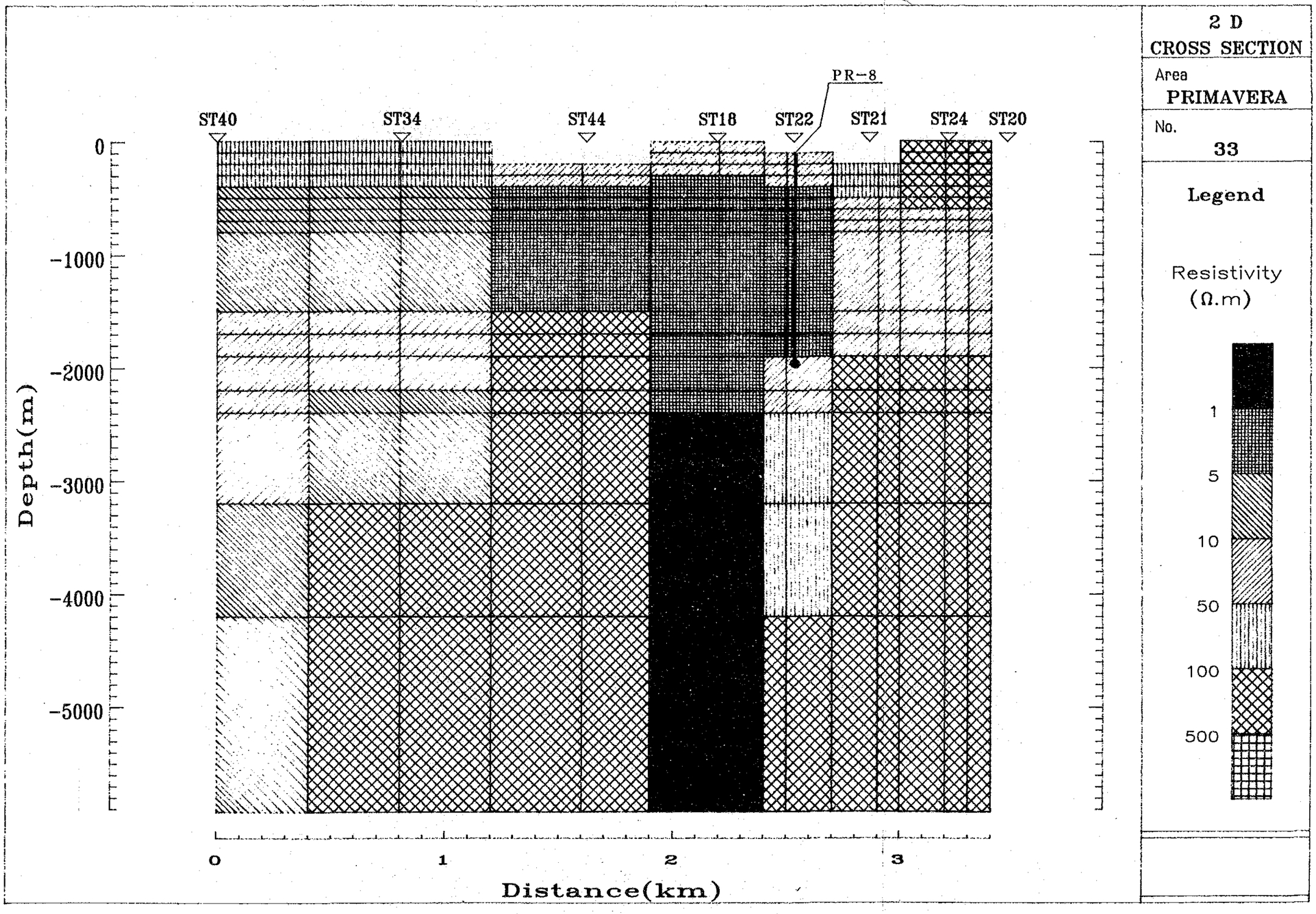

Fig. 39. 2-D model cross section, line 3.

Table 6. Recording band width, parameter and duration of MT survey

	Band width of freguency	Sampling Channel rate	Length of each recording segment	Segment number for 1 file	recording duration for 1 file	file number	Sampling number for FFT	Q value
HF	125Hz 3HZ	each 500Hz	512	64	about 1 min.	3～5	512	6
MF	15Hz 10second	each 60Hz	512	64	about 9 min.	3～5	512	6
LF	0.5Hz 200second	each 2Hz	512	30 40	130 170 min	1	1024	4

II-5 Well test

Downhole temperature and pressure under the dynamic state, namely the condetion of producing fluids from the wells, were measured on wells PR-1 and PR-8 from which steam blow out.

(1) Method and condition of measurement

The well tests conducted on wells PR-1 and PR-8 were to measure the temperature and pressure distribution in wellbore while producing the fluid, with respect to flow values set by adjusting well-heat value. The test must be done under pressurized condition of well-head. Insertion and removal of instruments into and from wellbone should, therefore, be made through a lubricator. The equipments used are Kuster thermometer and manometer connected with stainless wire of 5mm diameter.

In case of PR-1, judging from discharge condition from a 3 bread valve located under the main valve, both the permability and the fluid temperature were expected to be very high. As a result, 3 measurements were carried out using flow parameters as shown in Table 7 under consideration of insertion possibility of equipment. The first test was carried out under flow adjustment by 3 orifice and under full opening of 2nd valve. At that test, because of high flow and dryness rate, the fluid velocity in 4 1/2" casing became too high entraining a difficulty of apparatus insertion into the depth more than 1,150 m. Measurement was stopped at that depth. The second test was a simultaneous measurement of temperatuare and pressure by using 2" orifice, and the third test was a pressure measurement with orifice of 2 1/2"$^{\phi}$ opening diameter.

Geothermal fluid from PR-8 was directly discharged into the atmosphere without separator (steam, water). Accordingly, measurement was carried out only under this flow condition (Table 8).

(2) Results of PR-1 test

Table 9 and Fig. 40 show the temperature and the pressure in PR-1 wellbore. Based on these results, considerations on the wellbore condition of PR-1 are as follows.

(i) Relation between temperature and pressure shows a nearly saturated condition at each depth throughout the whole depth, forming thus two-phase flash flow entirely in the wellbore.

(ii) Fluid temperature reaches a very high value of 299 ℃ at 1,800 m near the bottom. Since the formation temperature reached 304-305 ℃ (according to C.F.E.) under a static condition at the same depth, the fluids appear to flow into the wellbore after flashing in the formation surrounding the well.

(iii) Concerning the change in pressure gradient between 1,400m and 1,450m, there might be 2 different conceptions as follows:

First conception is that the fluids are, after flashing in the formation, flowing into the annulus between the wall (7"$^{\phi}$) and the pierced casing pipe and into the wellbore itself independently, and then they become one flow at the depth of ca 1,440m above which no pierced pipe exists more.

Another thinking is based upon a joining of fluids from

former lost circulation fracture at 1,440m which seems to be still open even after clogging by cement. At the third measurement, the apparatus moved smoothly down in the 4 1/2" casing pipe as far as 1,420m. However, wire tension was loosened thereafter and further insertion was impossible even when the descent velocity was changed. As a result, attempts have been made by throttling the fully opened 2nd valve and increasing the descent velocity to pass the point. The attempts were successful and the wire reached the bottom after turning back the valve. According to the casing program, pierced pipes had installed starting from the point of 1,440m. The latter conception seems to be acceptable from the above experience.

(iv) Although the inflow point of fluids was not confirmed by the test, it must be any how in the vicinity of the bottom where lost circulation occurred during drilling. There must be a little water column at the bottom of the wellbore (deeper than the inflow point) according to contamination of the drawn up apparatus.

(3) Results of PR-8 test

Table 10 and Fig. 41 show results of PR-8 measurement. The following are the summary of well conditions based on the results.

(i) Temperatures and pressures at each depth are in a saturated relation from the wellhead upto 1,750m as ultimate descent of the apparatus. Accordingly, the flow condition in the wellbore should be a flashed two-phase similar to PR-1.

(ii) The fluid temperature is 231 ℃ and the pressure is 30.7 kg/cm² G at 1,750m. In a static condition, the temperature is more than 270 ℃ and the pressure is much higher than the above value (results by C.F.E.). This suggests that the fluids flow into the wellbore after flashing in the surrounding formation.

(iii) Because the apparatus could not go down beyond 1,750m, ca. 100m of a burried layer might be expected.

(4) Calculation of transmissivility

From the results of pressure measurement in PR-1 and PR-8, calculations of transmissibility on the surrounding formation have been carried out.

As mentioned above, the fluids from PR-1 and PR-8 are likely to flash in the formation, i.e. they are under two-phase flow condition. However, in case of the wells PR-1 and PR-8, the volume ratio of the steam to water is sufficiently high in the formation. Further, the pressure loss caused by flow in the fomration is mainly related with the voluminal flow. As a result, a equation of gas-phase flow has been applied for approximative calculation of transmissibility. Under the assumption of an adiabatic process at phase transformation, equation of radial flow of gas-phase can be expressed as under:

$$G = \frac{2\pi k h r_w (P_e^{1+m} - P_w^{1+m})}{(1+m)\mu_w \ell_n r_e / r_w \cdot p_w^m} \quad \cdots\cdots (1)$$

where G: steam flow rate kg/s

P_e: reservoir pressure at inflow depth kg/m²

P_w: pressure in wellbore at inflow depth — kg/m²

kh: transmissibility — m³

k: permeability — m²

h: effective thickness — m

γ_w: specific weight of fluid — kg/m³

μ_w: viscosity coefficient of fluid — kgs/m²

r_e: radius of influence area — m

r_w: radius of well — m

m: Polytrope index (saturated steam: 1.135)

According to equation (1), transmissibility can be calculated by equation (2) as under:

$$kh = \frac{(1+m)\,G\,\mu_w\,\ell_n\,r_e / r_w}{2\pi\gamma_w} \cdot \frac{p_w^{\,m}}{P_e^{\,1+m} - P_w^{\,1+m}} \quad \cdots\cdots\cdots\cdots \quad (2)$$

Putting the values from the twice measurements while producing the fluid in the equation:

$$kh = \frac{(1+m)\,\ell_n\,r_e / r_w}{2\pi\,(P_{w2}^{\,1+m} - P_{w1}^{\,1+m})} \cdot \left(\frac{G_1\,\mu_{w1}\,P_{w1}^{\,m}}{\gamma_{w1}} - \frac{G_2\,\mu_{w2}\,P_{w2}^{\,m}}{\gamma_{w2}}\right) \cdots\cdots \quad (3)$$

For determination of steam flows at the inflow point, converted values are applied under the assumption of iso-emthalpy transformation for flow in the wellbore on the basis of flow condition at well-head or in-line.

Table 11 and 12 show terms of calculation. Table 13 shows the results of calculation. Equation (3) is used for PR-1 and equation (2) for PR-8. As shown in Table 13, the permcability of

the fracture at PR-1 is higher than that at PR-8. However, if regarded as absolute value, the transmissibility being less than 1 darcy•m, they cannnot be judged to be good. In particular at PR-8, the fact that the apparatus could not go down more at ca.100m above the bottom (possibly burried) suggests a reduction in permeability. In spite of such moderate permeability at both PR-1 and PR-8, very powerful steams are produced. It might be attributed to the high fluid temperature.

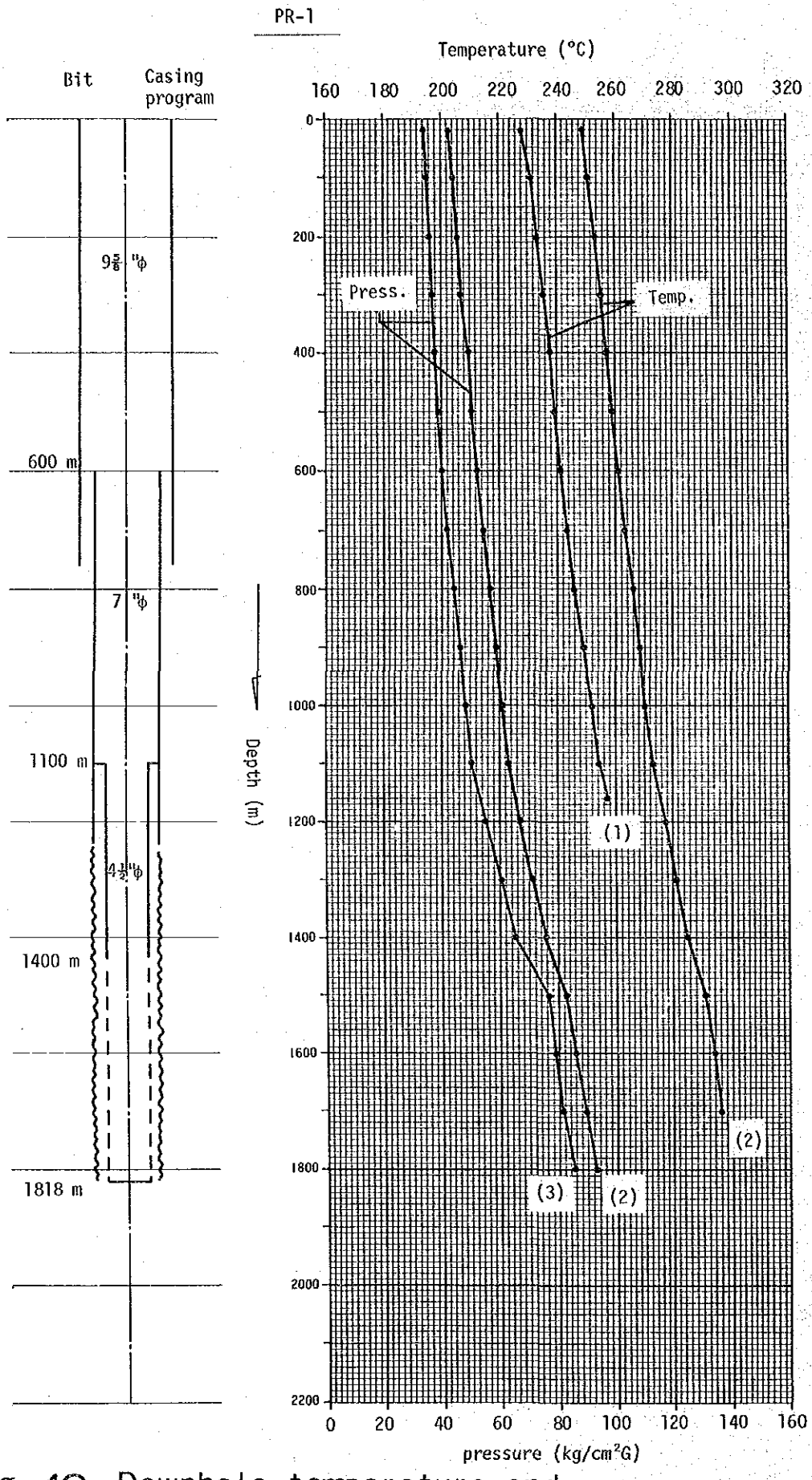

Fig. 40. Downhole temperature and pressure curves of PR-1 in the productive condition.

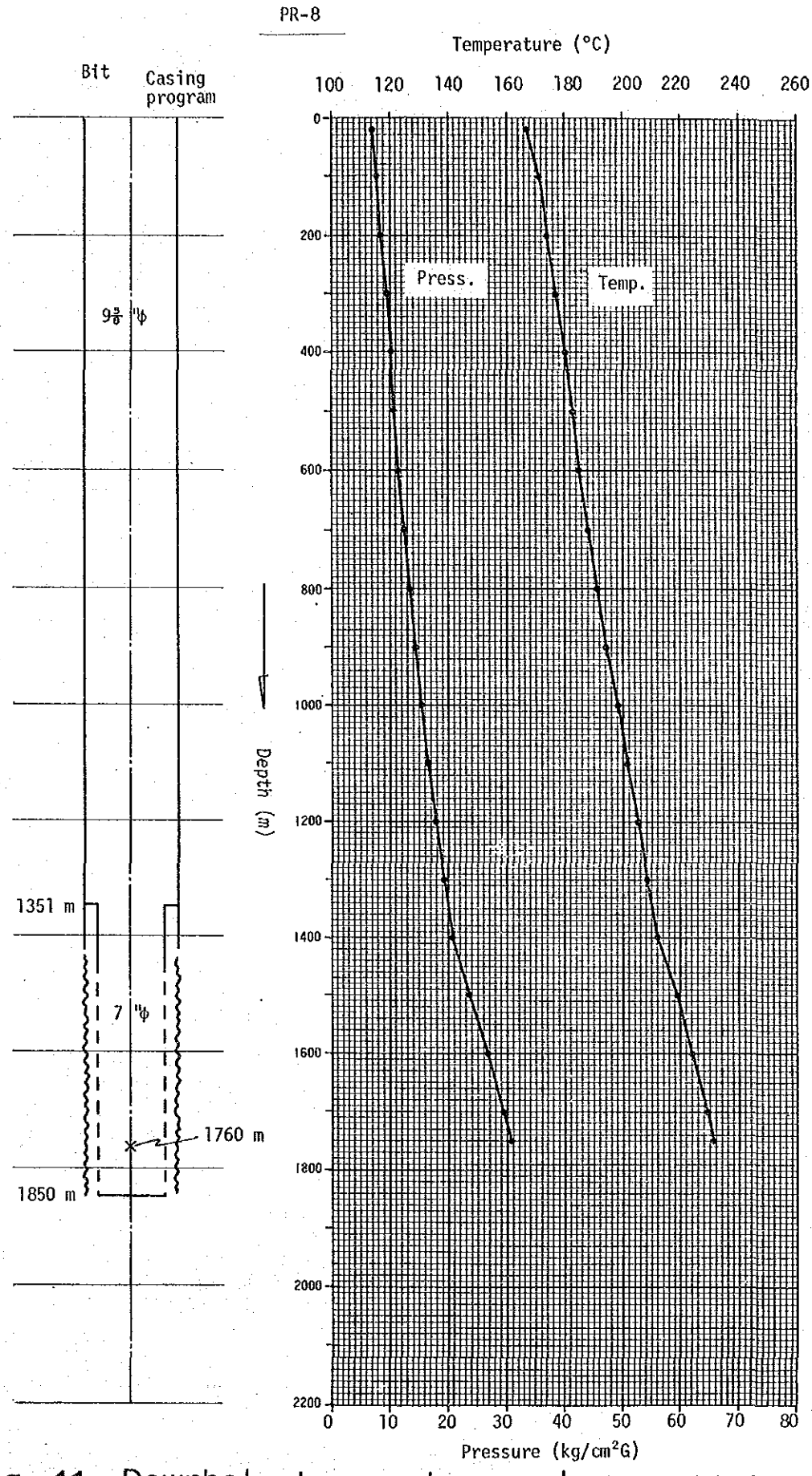

Fig. 41. Downhole temperature and pressure curves of PR-8 in the productive condition

Table 7. Situation of the well test for PR–1

	Measurement	Well head condition	Well head pressure	Flow rate	Quality at atmosphere
(1)	temperature	3"ϕ orifice 2nd valve: full open	28 kg/cm^{2}G	Gs = 53 t/h Gw = 51 G = 104 at atmosphere	0.31
(2)	temperature pressure	2"ϕ orifice 2nd valve: full open	42 kg/cm^{2}G	Gs = 43 t/h Gw = 40 G = 83 at line press.	0.25
(3)	pressure	$2\frac{1}{2}$"ϕ orifice 2nd valve: full open	36 kg/cm^{2}G	Gs = 50 t/h Gw = 47 G = 97 at line press.	0.27

Table 8. Situation of the well test for PR–8

	Measurement	Well head condition	Well head pressure	Flow rate	Quality at atmosphere
(1)	dummy temperature	2nd valve: full open	7 kg/cm^2	Gs = 45 t/h Gw = 60 G = 105 at atmosphere	0.29
(2)	temperature and pressure	idem.	idem.	idem.	idem.

Table 9. Results of measurement for PR-1

Date	7. Feb. 1986	8. Feb. 1986		10. Feb. 1986
Well depth	1818 m			
Well head condition	3"ϕ orifice	2"ϕ orifice		$2\frac{1}{2}$"ϕ orifice
Well head pressure	28 kg/cm^{2}G	41.5 ∿ 43		36
Depth (m)	Temperature(°C)	Temp.	Pressure(kg/cm^2)	Press.
20	228	249	42.2	34.1
100	231	251	44.0	35.0
200	233	253	45.7	36.0
300	235	255	47.3	37.0
400	237	257	48.9	38.1
500	239	259	50.4	39.1
600	241	261	52.1	40.2
700	243	263	54.2	42.1
800	245	266	56.3	44.2
900	249	268	58.4	46.3
1000	252	270	60.7	48.4
1100	254	273	62.9	50.4
1160	257			
1200		277	67.2	55.3
1300		281	71.5	60.5
1400		285	75.8	65.6
1500		291	82.7	76.4
1600		294	85.9	79.1
1700		296	89.2	81.8
1800		299	92.5	84.8

Table 10. Results of measurement for PR-8

Date	30. Jan. 1986	31. Jan. 1986	
Well depth	1861 m		
Well head condition	2nd valve: full open	2nd valve: full open	
Well head pressure	7.0 kg/cm^{2}G	7.0	
Depth (m)	Temperature(°C)	Temp.	Pressure(kg/cm^2)
20	167	166	7.1
100	171	170	7.9
200	174	173	8.4
300	177	176	9.4
400	180	179	10.1
500	183	182	10.8
600	185	185	11.5
700	188	188	12.4
800	191	191	13.3
900	194	194	14.2
1000	198	197	15.3
1100	201	200	16.5
1200	205	204	17.8
1300	208	208	19.2
1400	212	211	20.8
1500	219	218	23.8
1600	224	224	26.8
1700	229	228	29.2
1750	231	231	30.7

Table 11. List of parameters used in calculation of kh for PR-1

	1st step well head press. 42 kg/cm²G total flow rate 83 t/h	2nd step well head press. 36 kg/cm²G total flow rate 97 t/h
Pressure at feed point Pw kg/cm²G	92.5	84.8
Steam flow rate at feed point G t/h	20.4	26.5
Specific gravity of fluid at feed point γ_w kg/m³	49.9	45.1
Viscosity coefficient of fluid at feed point μ_w kgs/m²	2.18×10^{-6}	2.15×10^{-6}

Table 12. List of parameters used in calculation of kh for PR-8

	Static test	Production test well head press. 7 kg/cm^{2}G total flow rate 105 t/h
Pressure at feed point Pw kg/cm^{2}G	123	30.7
Steam flow rate at feed point G t/h	—	21.5
Specific gravity of fluid at feed point γ_w kg/m^3	—	15.6
Viscosity coefficient of fluid at feed point μ_w kgs/m^2	—	1.82×10^{-6}

Table 13. Results of calculation of kh

Well	kh (m^3)
PR-1	7.6×10^{-13}
PR-8	2.1×10^{-13}

II-6. Comprehensive analysis on geothermal reservoir

(1) Stracture of geothermal reservoir

It could be concluded that NE-SW oriented fractures dominating in shallow subsurface extend up to the depth of about 1,000m, while fractures existing at deeper than 1,000m show NE-SE direction. This fracture system was formed by resurgent uplift occurred after depression of Sierra La Primavera Caldera and it became clear that the center of uplift is located near PR-1 and PR-8. Geothermal manifestations such as fumaroles and rock alteration zones are distributed along fractures with NE-SW direction.

On the other hand, lost circulations during drilling of PR-1 and PR-8 are caused by encounter to the deep seated fracture with NW-SE direction.

The upflow zone of high temperature fluid is recognized between PR-1 and PR-8, judging from the profile of underground temperature obtained from well test and fluid inclusion. The ascending deep hot water is diluted by underground water reserved in fractures with NE-SW direction in flowing from PR-1 to PR-4 through PR-8 and PR-5. Hot water of PR-2 is considered to be derived from another separated reservoir.

From the fact mentioned above, it can be said that both the uplifted zone and upflow zone are existed near PR-1 and PR-8, forming vertical fracture type geothermal reservoir. This is also supported by the electrical survey result (MT method) that the low resistivity zone extends to deep subsurface at southern part of PR-8 (sounding station 18).

(2) Extent of geothermal reservoir

Extent of geothermal reservoir in this area is estimated as follows:

PR-9 located about 300m west of PR-1 which has temperature of 305 ℃ at depth of 1,800m was drilled to 2,986m in depth and reached the "basement rocks". However, the hole temperature did not rise up above 240 ℃ and encountering no significant circulation losses. Then, PR-10 was drilled up to 1,250m on the location of about 600m north of PR-8, showing maximum hole temperature of 144 ℃. These facts suggest that geothermal fluid is reserved only in vertical fractures and no high temperature nor rock permeability can be obtainable at outside of the fracture zone because of vertical fracture type geothermal reservoir.

Fig. 42 shows the deep fracture zone with NW-SE trend related to the upflow zone and the shallow fracture system with NE-SE trend, based on the analysis so far obtained. The deep fractures with NW-SE trend, although not clear on the surface, are evident from the MT method results, while the shallow fractures with NE-SW trend are supported by existence of hydrothermal rock alteration and so on. Because of dilution of hot fluid with surface water, it is doubtful whether the shallow fractures produce steams with high enthalpy.

It is concluded that geothermal development will not be feasible at outside area of the fracture zone, since geothermal reservoir is characterized by vertical fracture in this area.

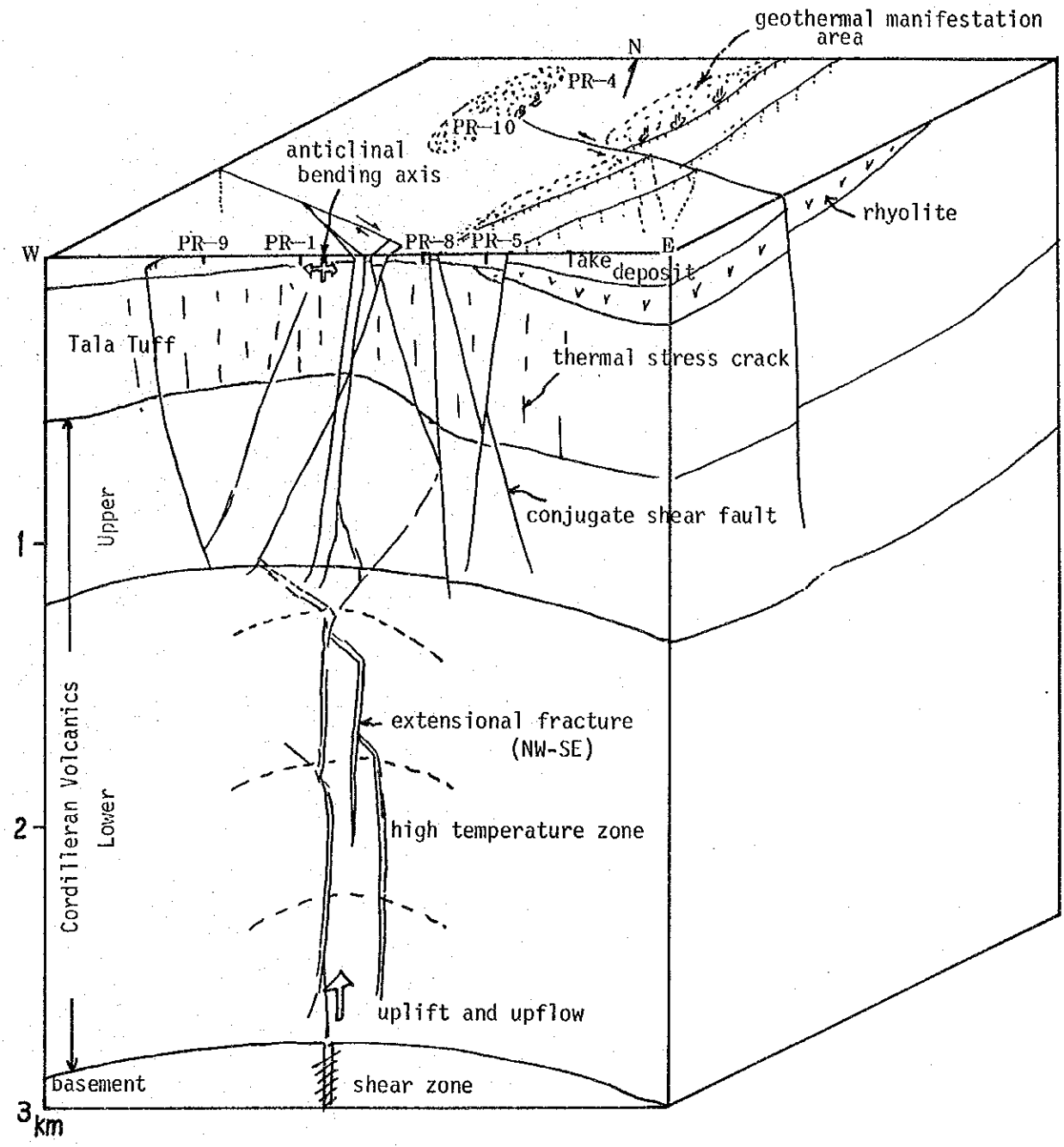

Fig. 42. Conceptual geothermal reservoir model in La Primavera

Ⅲ. Proposal for the work plan of next stage

III. Proposal for the work plan of next stage

Geological, geochemical, gravimetric and electrical (MT method) surveys and well testing, in addition to review of the data on the exploration wells, have been carried out in FY 1985. From the results of comprehensive analysis of data, it has become clear that the geothermal reservoir in La Primavera is controlled by location of an uplifted zone which plays a role as an upflow zone of geothermal fluid with high fluid temperature.

According to the scope of work of the Project, it is scheduled that three heat holes of 750m in depth will be drilled by C.F.E. in FY 1986. However, for the following reasons, it is better to change the work plan in FY 1986 to drill one exploration well of about 2,000m in depth in exchange of drilling of three heat holes.

1. According to the investigation in FY 1985, the upflow zone and the distribution of underground temperature are now clarified.
2. Seven wells (600～3,000m in depth) had already been drilled by C.F.E, and the thermal extention is already known.
3. Because of thick sedimentation of Tala Tuff up to about 700m depth which caused frequent lost circulations, it would take for long time to drill through the formation.

So that, it is more important for collecting useful data to evaluate the geothermal reservoir that a new deep well would rather be drilled toward the upflow zone than drilling of heat

holes.

Another exploration well will be drilled by JICA study team in the manner of directional drilling in FY 1987.

III.-1. Purpose of drilling of exploration wells

Up to the present, only two exploration wells (PR-1 and PR-8) were drilled through the upflow zone in which fracture well develop, but other exploration wells (PR-2,5,9 and 10) were located at outside of the upflow zone. In order to determine the optimum output of the planned power station by delineating geothermal reservoir, it is necessary to evaluate the potential of upflow zone. The purpose of drilling of exploration wells is to collect useful data of the upflow zone to estimate the geothermal reservoir.

III-2. Reasons for selection of targets

For this purpose, two targets, points A and B shown in Fig.43, were selected for exploration wells which will be drilled on and after FY 1986. Each target must be a point necessary for determining the extent of developing area and the output of the planned geothermal power station by using the data of two exploration wells in addition to PR-1 and PR-8.

The reason that A and B points were selected is shown as follows:

Both points A and B are

(1) Necessary points to detect the extent of geothermal reservoir

(2) Located of an upflow zone

(3) Located on possible deep seated fractures

Point A is

(1) Located on horst estimated from the distribution of surface faults (Fig. 3),

(2) Located on tensional fracture concentrated zone obtained from tensional fracture distribution map on the surface (Fig. 5).

Point B is

(1) Located on low resistivity zone extending vertically near the station 18 found by MT method.

(2) Located on an anticlinal bending axis restored by the stress field (Fig. 4)

(3) Located on maximum upheaval zone of giant pumice bed

As to selection of the targets for drilling of exploration wells, C.F.E. has accepted the method of aiming at specific faults which are only recognized at the surface and are extended to the subsurface without physical consideration. This method is valied in the case of having large throw of fault and homogeneous formation from the surface to the deeper subsurface. However, in Sierra La Primavera the subsurface geology is different from the surface geology in the orientation of fracture and fracture characteristics. Moreover, the fracture behavior is easily changeable in high temperature and high pressure at the subsurface (see References). Therefore, it is better to select the targets by comprehensive analysis of various surveys with a consideration of deep seated fracture than by making a great point of only surface geology.

Point A has about 200m distance away from PR-1 and about

250m from PR-8, while point B has about 300m distance away from PR-1 and about 270m from PR-8. However, it has no problem on scrambling of fluid among production wells because both A and B points are inside the upflow zone where excellent geothermal fluids are provided from the deeper subsurface.

III-3. Survey plan of drilling of exploration wells

It is scheduled that point A is Drilled by C.F.E. in FY 1968 and point B is drilled by JICA in FY 1969. We call tentatively point A PR-11 and point B PR-12, showing well layout in Fig. 44 and undertaking for wells in Table 14 respectively.

As to the drilling of PR-12 well, the following method may be proposed;

1) vertical drilling at newly prepared drilling site
2) side-tracking of PR-5 or R-9 well
3) controlled directional drilling from the platform of PR-8 well.

The final decision about which method is employed will be done after the analysis of the result of the drilling of PR-11 well.

References

1) K. Sato, et al., "Breakdown pressure prediction in hydraulic fracturing at the Nigorikawa geothermal field", Hydraulic fracturing and geothermal energy, 1983 Martinus Nijhoff Publishers.

2) M. Takanohashi, et al., "Evaluation of rock fracture toughness in the presence of pressurized water at elevated temperature by means of AE technique", Progress in Acostic Emission II, Proceedings of The 7th International Acostic Emission Symposium, The Japanese Society for Non-Destructive Inspection (1984)

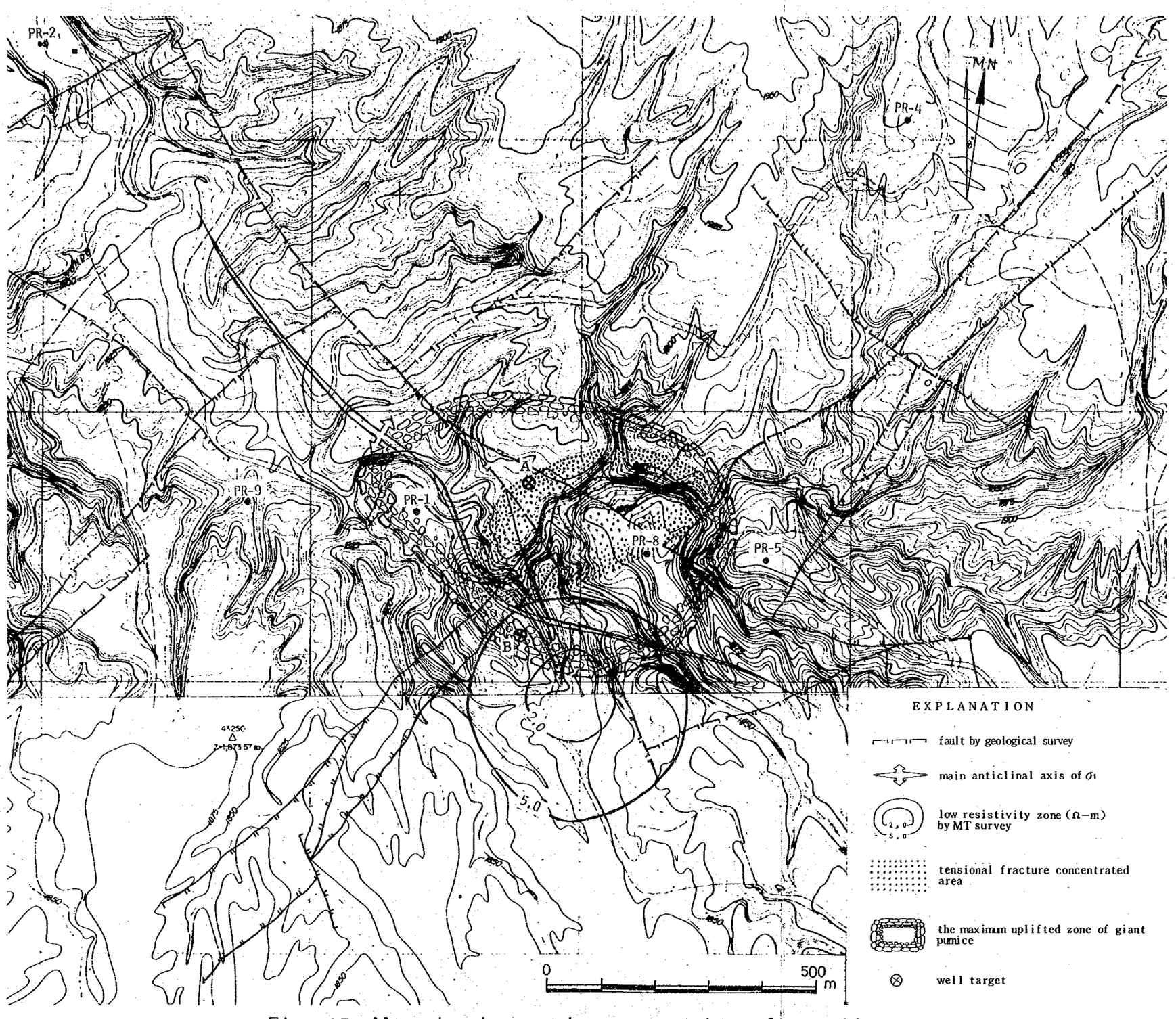

Fig. 43. Map showing various parameters for well target selection

PR-11 (well target A)

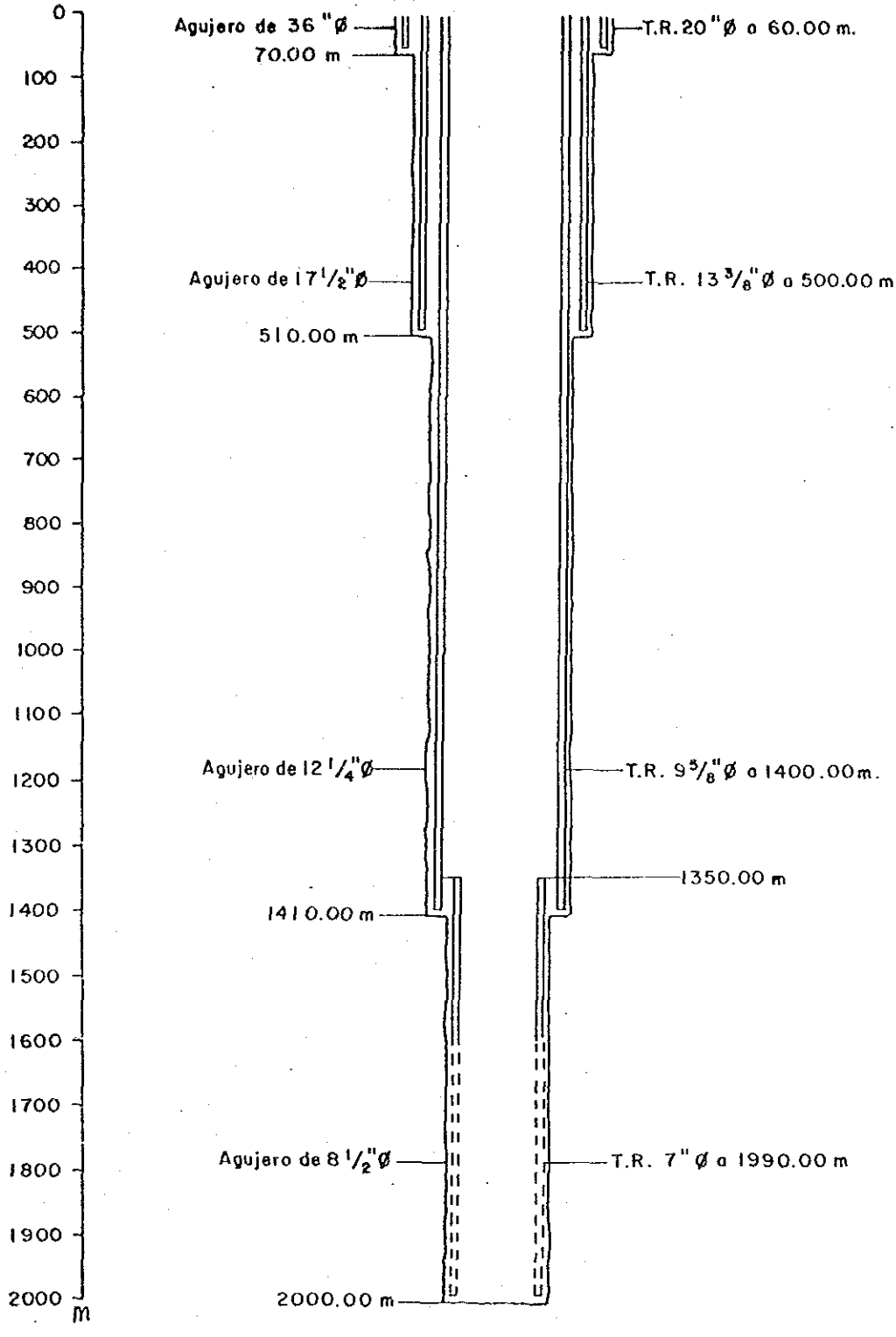

Fig. 44. Well layout of PR-11

Table 14. Respective undertaking for the exploration wells

Well	JICA	CFE
PR-11	1.Determination of the well position and completion depth 2.Analysis of fluid inclusion, X-ray and Hg,As concentration of cuttings 3.Physical property and fracture analysis of cores 4.Chemical analysis and geophysical test of wellbore fluid which will carry out after the finish of PR-12 well.	1.Drilling works 2.Core sampling at 1400, 1700 and 2000 m (each 1-3m long of core) 3.General geological survey 4.Downhole temperature and pressure logging 5.Measurement of physical characteristics of geothermal fluid
PR-12	1.Determination of the well position and completion depth 2.Supervision of the drilling work 3.Payment of the contract value 4.Analysis of cuttings and cores 5.Chemical analysis and geophysical test of wellbore fluid together with PR-11 6.Analysis and evaluation of the results	1.Drilling works 2.General geological survey 3.Downhole temperature and pressure logging 4.Measurement of physical characterristics of geothermal fluid

Concise summary

CONCISE SUMMARY

Geological, geochemical, gravimetric and electrical (MT method) surveys and well testing have been carried out in Sierra La Premavera in FY 1985. From the results of comprehensive analysis of data, it has become clear that the fractures up to about 1,000 deep consist mainly of the NE-SE trend normal fault system which is consistent with the NE-SW structure obtained from hydrothermal rock alteration, mercury concentration in soil, relation of the enthalpy with Cl^--concentration and gravimetric survey. On the contrary, the fracture pattern for depth more than 1,000m has been assumed to be high angle extensional fractures with NW-SE trend, based on the structural analysis of the "basement rocks" and Tertiary System and on the orientation of low resistivity zone by an electrical survey (MT method). The fracture system is formed by resurgent uplift after Sierra La Primavera Caldera forming, and the center of uplift is located near PR-1 and PR-8 wells.

A high temperature upflow zone is situated in the vicinity of PR-1 and PR-8, judging from the results of downhole temperature measurements, minimum homogenization temperature of fluid inclusion and chemical composition of wellbore fluid.

This geothermal area is characterized by a vertical reservoir with uplift zone that is neary coincided with the upflow zone.

In order to determine that optimum output of the planned power station by delineating geothermal reservoir, it is necessary to drill two exploration wells (2,000m in depth) in

addition to PR-1 and PR-8 through the upflow zone which provides useful data for estimate the geothermal reservoir. For this purpose, two targets were selected for exploration wells. One exploration well is an exchanged one for drilling of three heat holes of 750m in depth in FY 1986.

APPENDIX

Original data of the remanent magnetization and the restoration of principal stress axis by cores

①

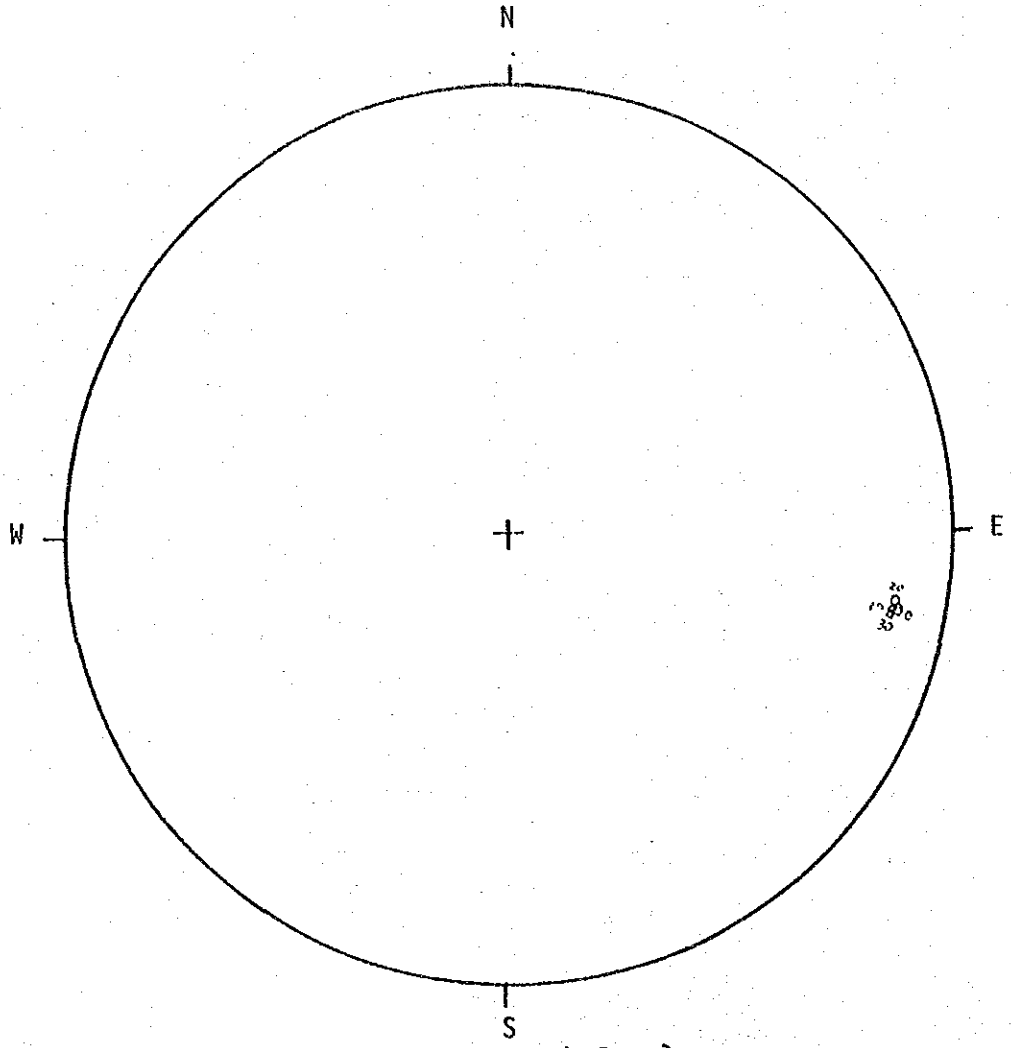

AF demag. mT ▲ △ before } bedding correction
MW demag. min. ● ○ after }
Susceptib. mA ⊙ Max. ○ Int. □ Min.

Sample Name	NRM(kA/m)		Jn(kA/m)	Jsus(kA/m)	$\frac{J_{B.Max}}{K_{33}}$(kA/m)	qn
MXPR15MA	2.2±E-3			1.76E-4	± 1.0	
(PR-1, 93m)		10%	2.2±E-3	2.14E-4	± 1.1	
		20%	2.21E-3	1.98E-4	± 0.8	
		30%	2.0×E-3	1.78E-4	± 0.8	

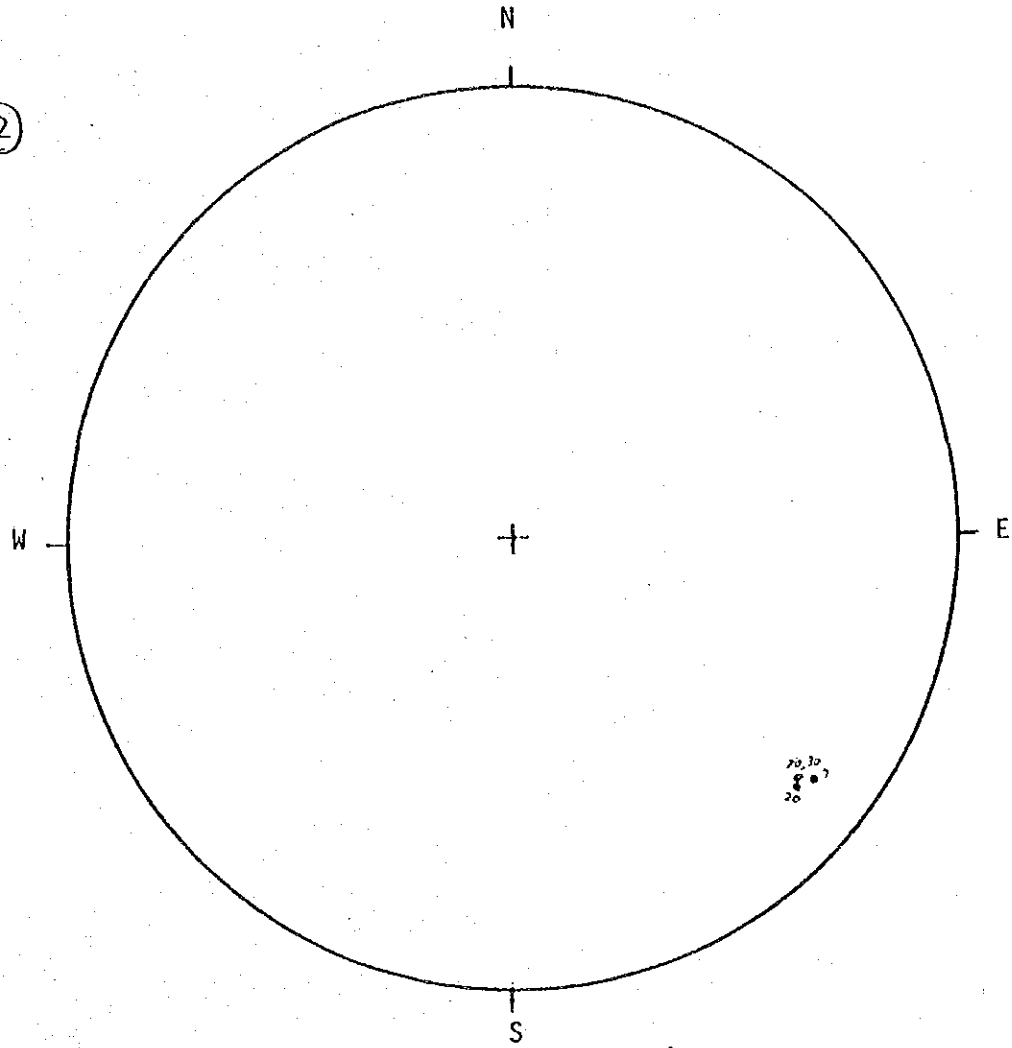

② 20,30

AF demag. mT
MW demag. min.
Susceptib. mA

▲ △ before } bedding correction
● ○ after }
◎ Max. ○ Int. □ Min.

Sample Name	NRM(kA/m)	Jn(kA/m)	Jsus(kA/m)	$J_{B\,min.}/K_{33}$(kA/m)	qn
MXPR IIMA	2.29E-3.		2.83E-4	±0.5	
(PR-1, 910m)		10_{mT} 2.31E-3	2.63E-4	±0.7	
		20_{mT} 2.28E-3	2.28E-4	±0.5	
		30_{mT} 2.07E-3	2.14E-4	±0.5	

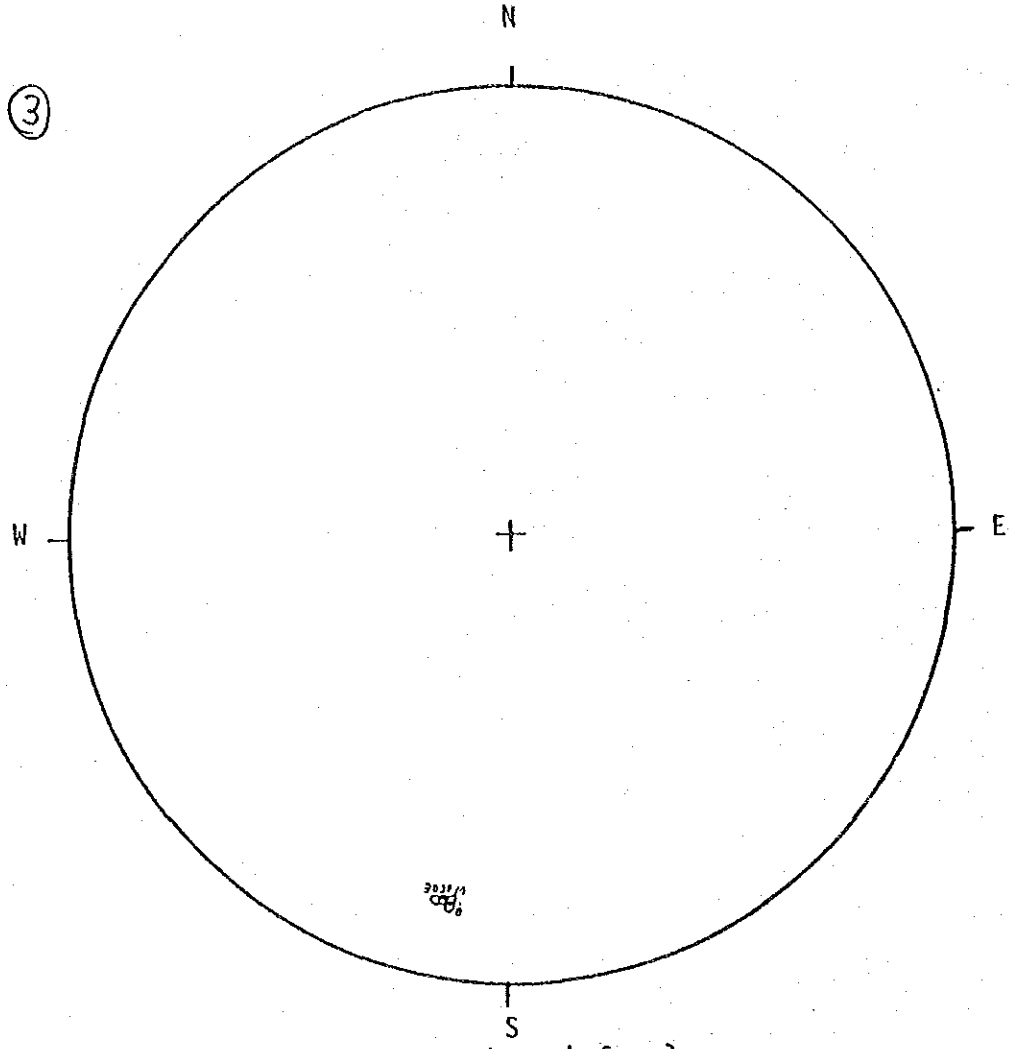

AF demag. mT ▲ △ before } bedding correction
MW demag. min. ● ○ after }
Susceptib. mA ⊙ Max. ○ Int. □ Min.

Sample Name	NRM(kA/m)	Jn(kA/m)	Jsus(kA/m)	$J_{B\ error}$ / K_{33}(kA/m)	qn
MXPR13MA (PR-1, 915m)	1.49E-3		5.76E-5	±1.9	
	10mT	1.52E-3	5.10E-5	± 2.0	
	20mT	1.50E-3	5.19E-5	± 2.0	
	30mT	1.43E-3	5.84E-5	± 1.7	

④

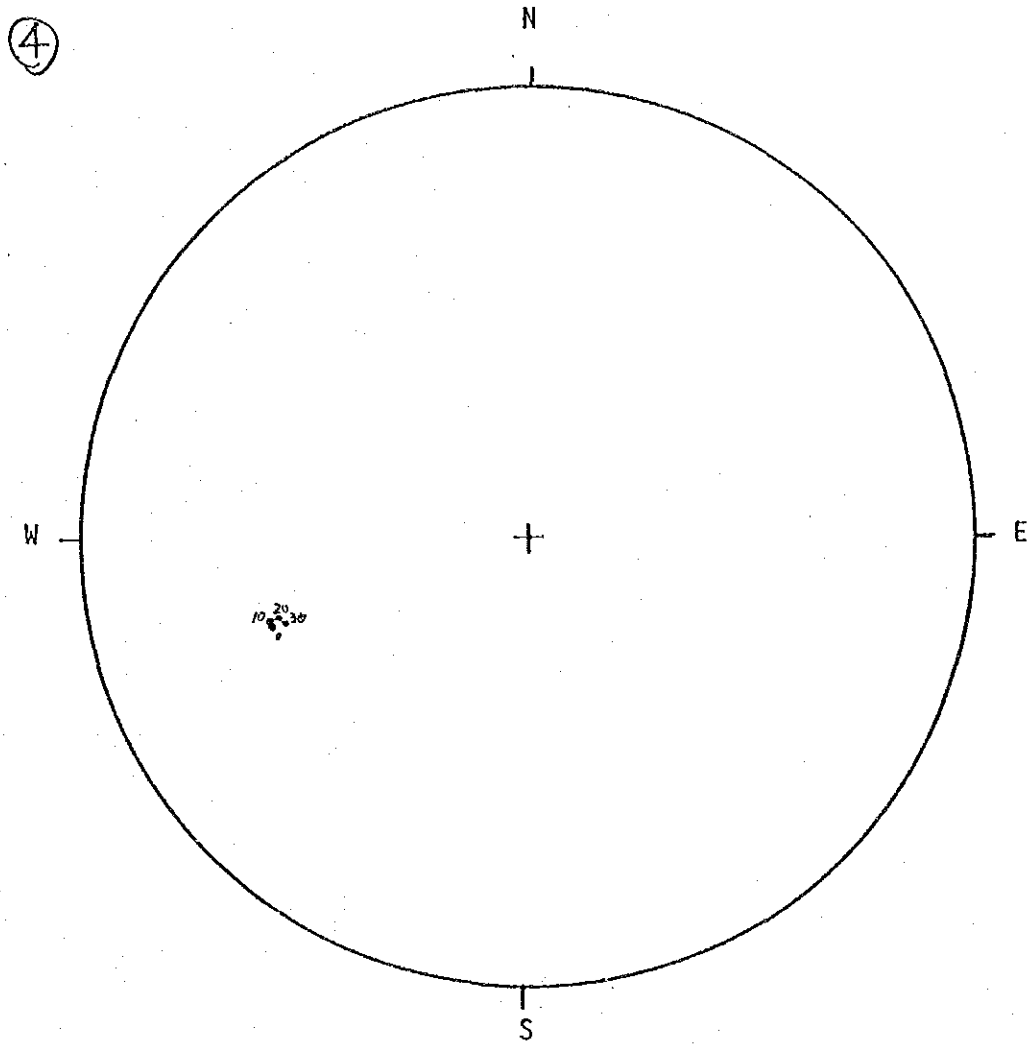

AF demag. mT ▲ △ before } bedding correction
MW demag. min. ● ○ after }
Susceptib. mA ⊙ Max. ○ Int. □ Min.

Sample Name	NRM(kA/m)	Jn(kA/m)	Jsus(kA/m)	$J_{B.max.}$ / $\overline{K_{33}}$(kA/m)	qn
MX PR28MA	2.9E-3		1.46E-4	± 1.0	
(PR-2, 350m)		10 mT 2.90E-3	1.48E-4	± 1.1	
		20 mT 2.21E-3	1.18E-4	± 1.1	
		30 mT 1.22E-3	4.46E-5	± 1.0	

⑤

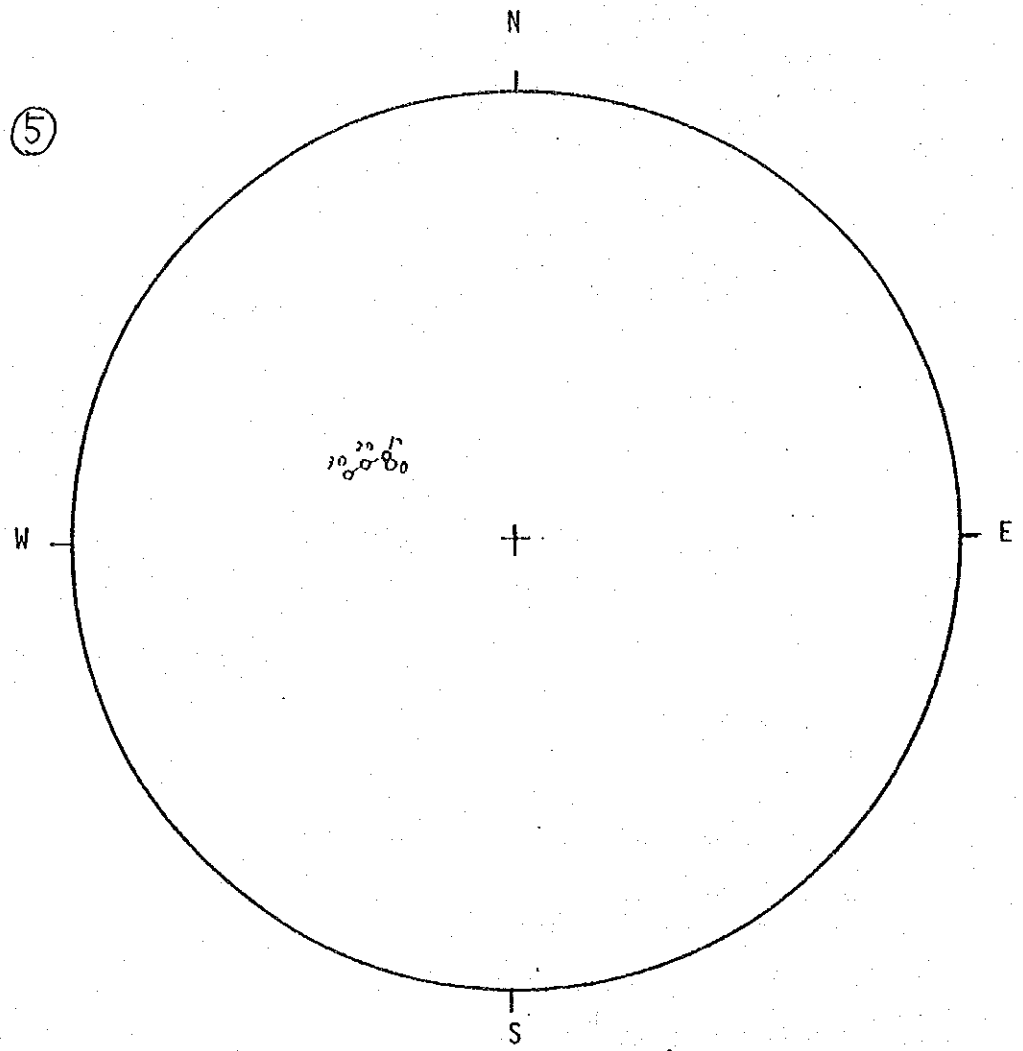

AF demag. mT ▲ △ before } bedding correction
MW demag. min. ● ○ after }
Susceptib. mA ⊙ Max. ○ Int. □ Min.

Sample Name	NRM(kA/m)	Jn(kA/m)	Jsus(kA/m)	K_{33} (kA/m)	$I_{95\%error}$	qn
MXPR24MA (PR-2, 1360m)	7.47E-4		6.91E-5		±1.2	
		10_{mT} 6.86E-4	7.47E-5		±1.0	
		20_{mT} 5.43E-4	5.82E-5		±1.2	
		30_{mT} 3.48E-4	3.62E-5		±1.1	

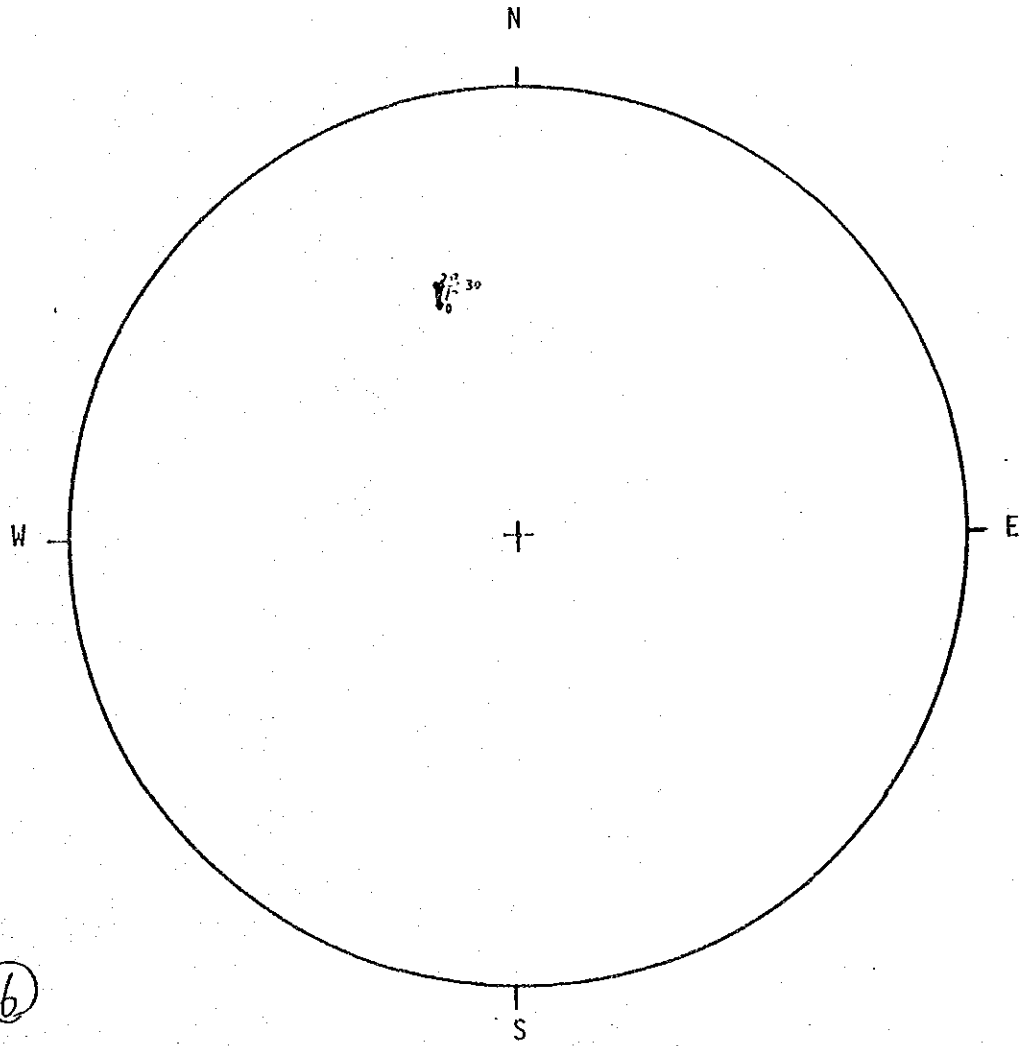

(6)

AF demag. mT ▲ △ before } bedding correction
MW demag. min. ● ○ after }
Susceptib. mA ⊙ Max. ○ Int. □ Min.

Sample Name	NRM(kA/m)	Jn(kA/m)	Jsus(kA/m)	$J_{R\,error}$ / K_{33}(kA/m)	qn
MXPR46MA	4.17E-4		2.61E-3	± 0.9	
(PR-4, 300M)		10mT 3.51E-4	3.49E-3	± 0.6	
		20mT 2.86E-4	2.07E-3	± 0.7	
		30mT 2.26E-4	1.52E-3	± 0.5	

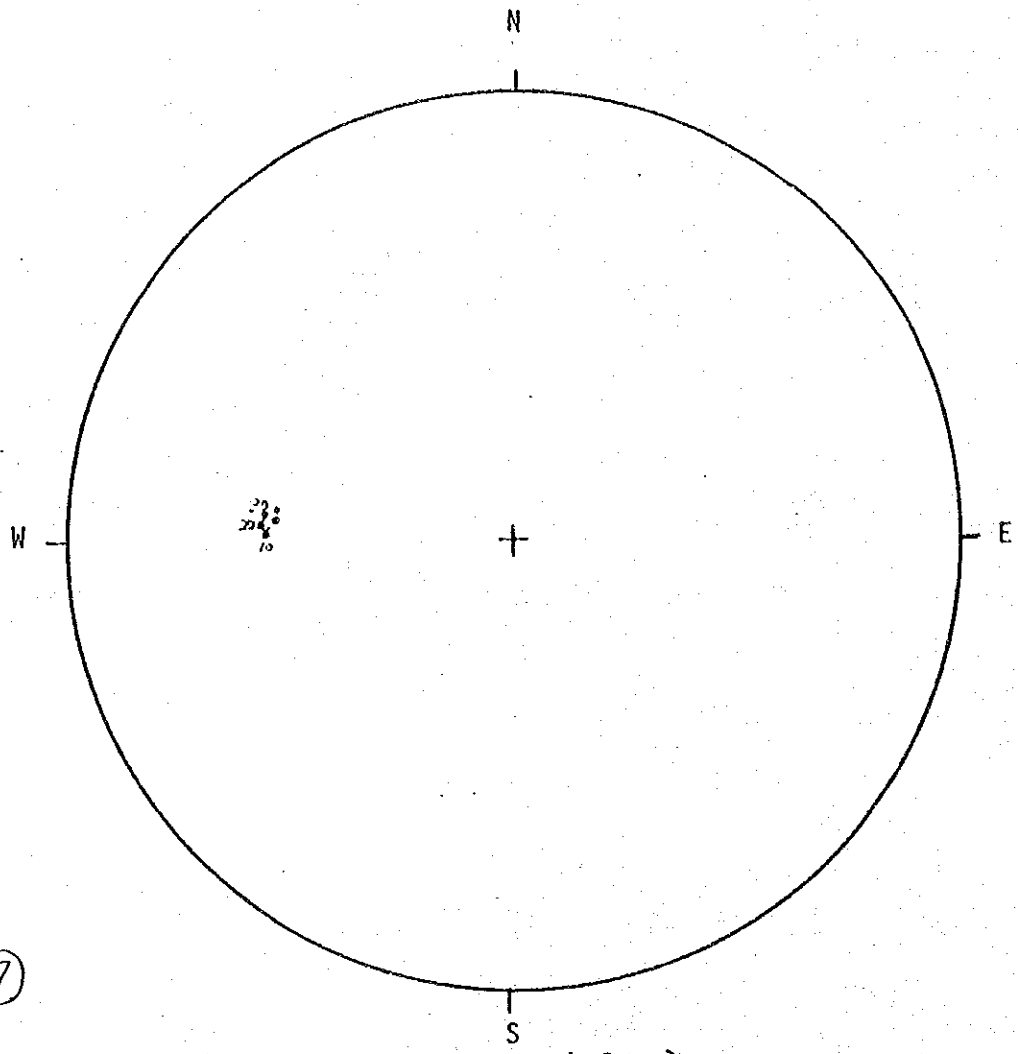

⑦

AF demag. mT ▲ △ before } bedding correction
MW demag. min. ● ○ after }
Susceptib. mA ⊙ Max. ○ Int. □ Min.

Sample Name	NRM(kA/m)	Jn(kA/m)	Jsus(kA/m)	$J_{B\text{-}min}/K_{33}$(kA/m)	qn
MXPR5-7MA	4.17E-4		6.08E-3	±1.3	
(PR-5, 350m)		10_{m-1} 3.43E-4	3.62E-3	±1.2	
		20_{m-1} 2.48E-4	2.29E-3	±1.1	
		30_{m-1} 2.07E-4	2.13E-3	±1.3	

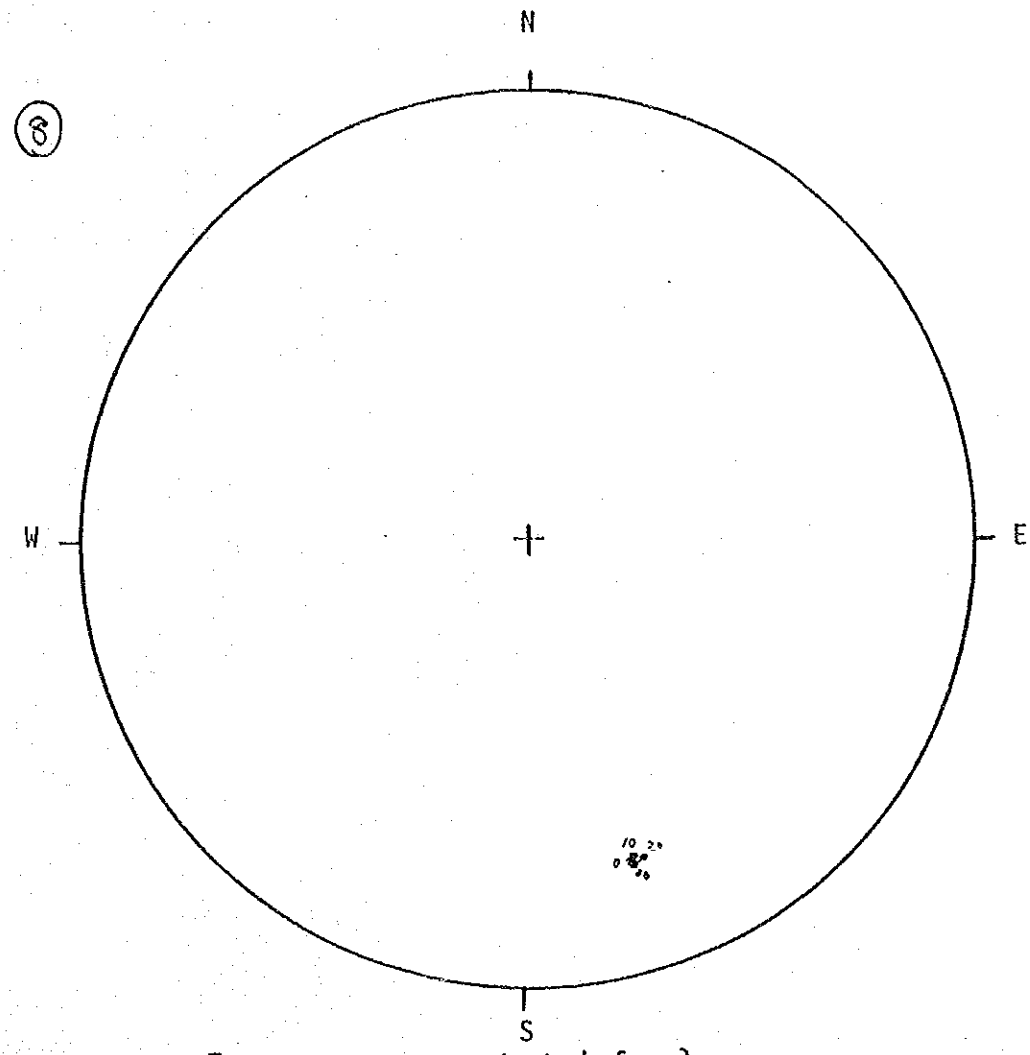

AF demag. mT
MW demag. min.
Susceptib. mA

▲ △ before
● ○ after
} bedding correction

⊙ Max. ○ Int. □ Min.

Sample Name	NRM(kA/m)	Jn(kA/m)	Jsus(kA/m)	$K_{33}^{I_{Bedding}}$(kA/m)	qn
MX RC12MA	9.24E-3		6.99E-4	± 0.4	
(RC-1. 700m)					
	10_{mT}	9.18E-3	6.82E-4	± 0.5	
	20_{mT}	8.63E-3	4.79E-4	± 0.1	
	30_{mT}	7.12E-3	1.12E-4	± 0.1	

① PR-1, 93m

vein

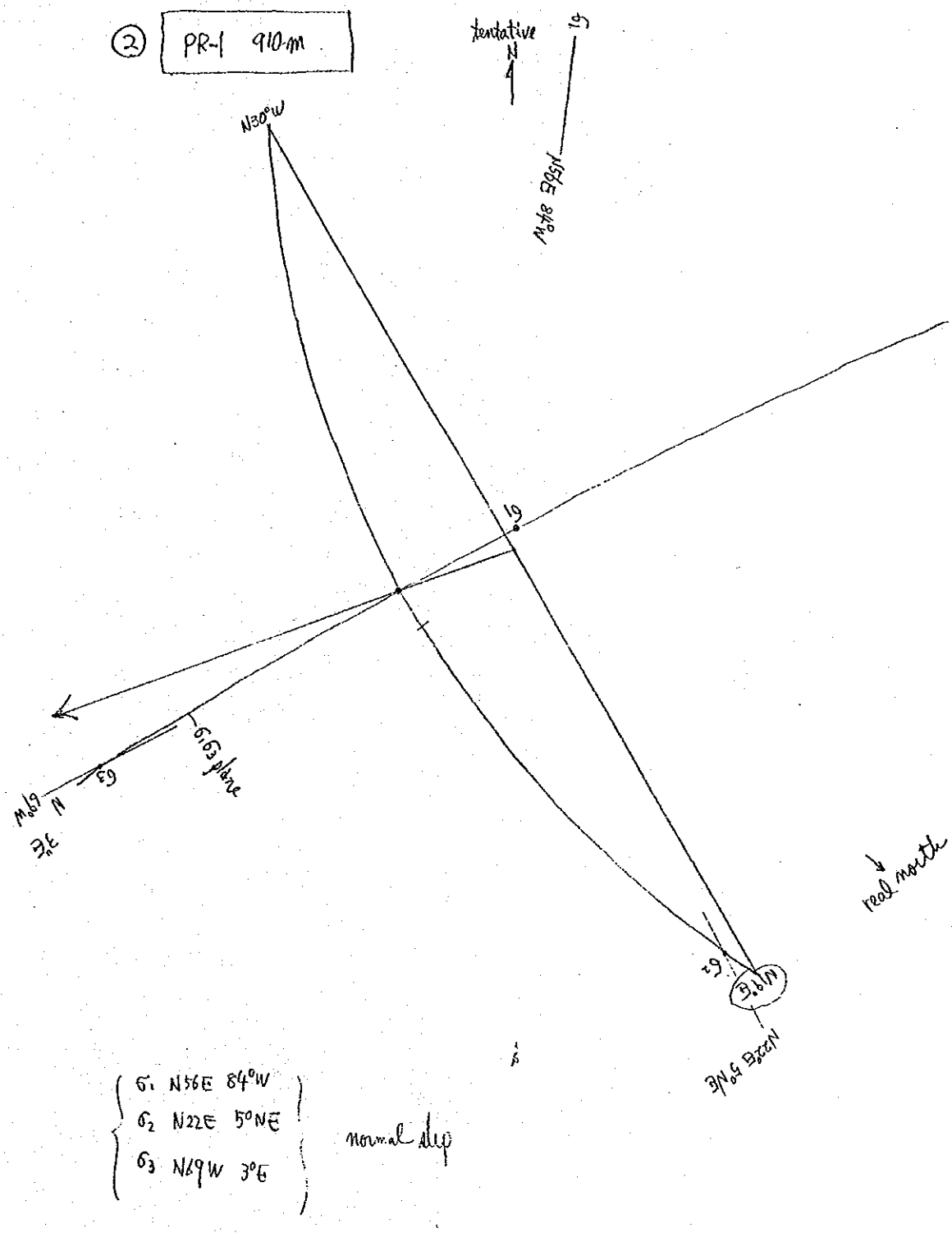

σ_1 N56E 84°W
σ_2 N22E 5°NE
σ_3 N69W 3°E

normal dip

③ PR-1 915m

tentative N
true/real south
G1 N66°E 86°W
G2 N11°W 2°N
G3 N78°E 3°E
G1 N66°E 86°W
pool route
south
N12°W
G2 N11°W 2°N
G3 N78°E 3°E

"

slickenside direction → vertical

④ PR-2, 350m

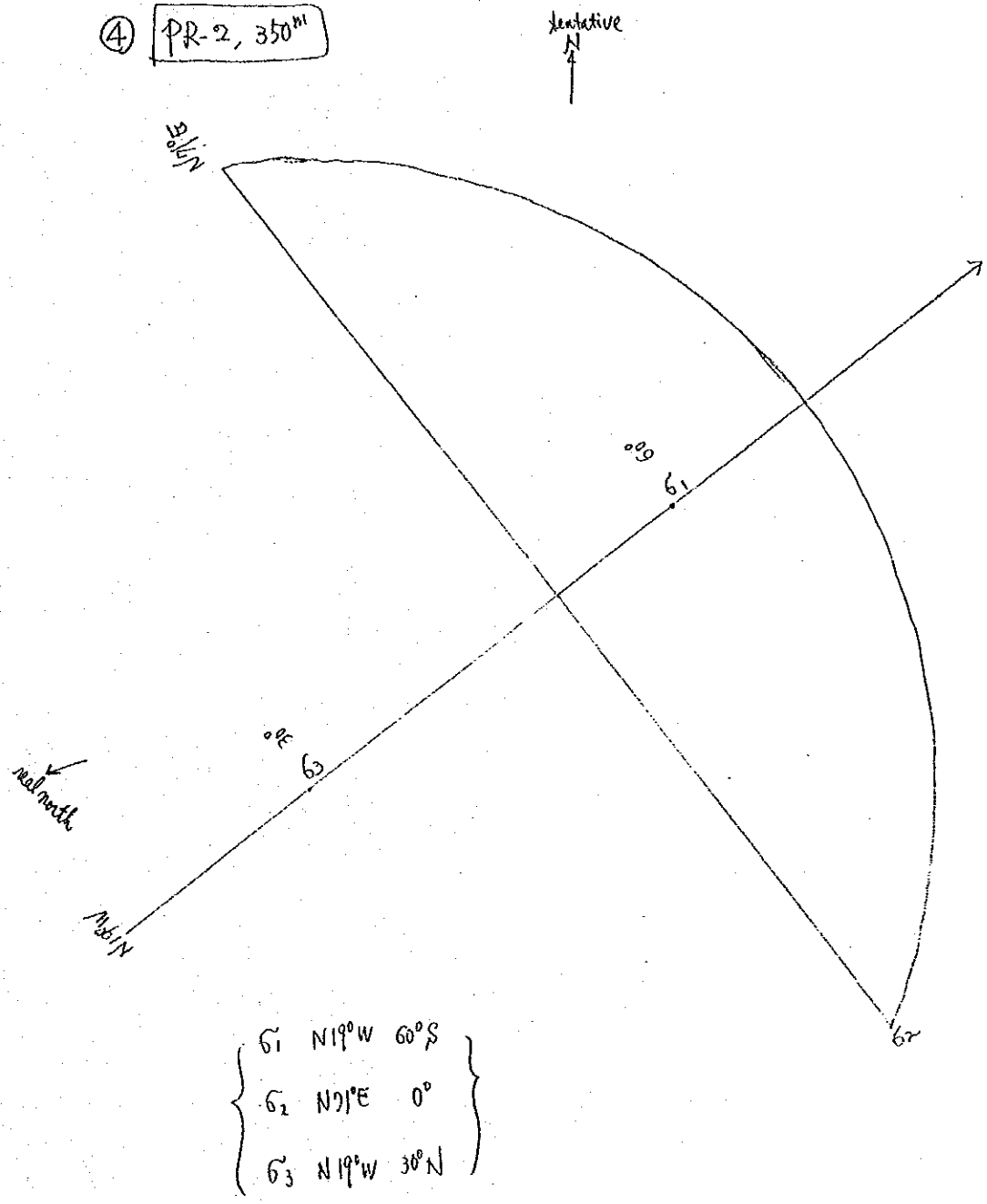

σ_1	N19°W	60°S
σ_2	N71°E	0°
σ_3	N19°W	30°N

⑤

PR-2
1,360m

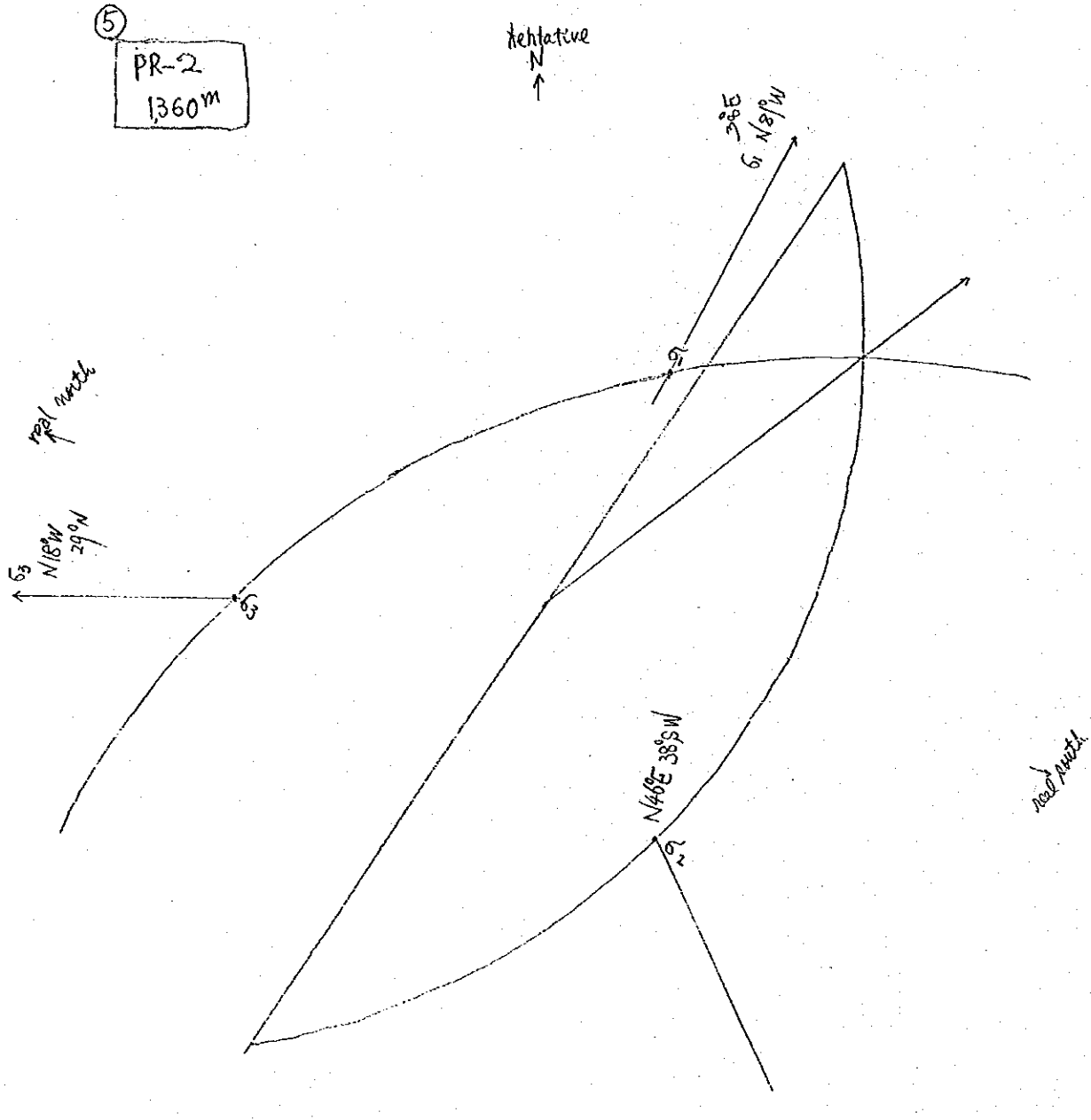

σ_1	N 81°W	38°E	Complete Oblique
σ_2	N46°E	38°SW	
σ_3	N18°W	29°N	

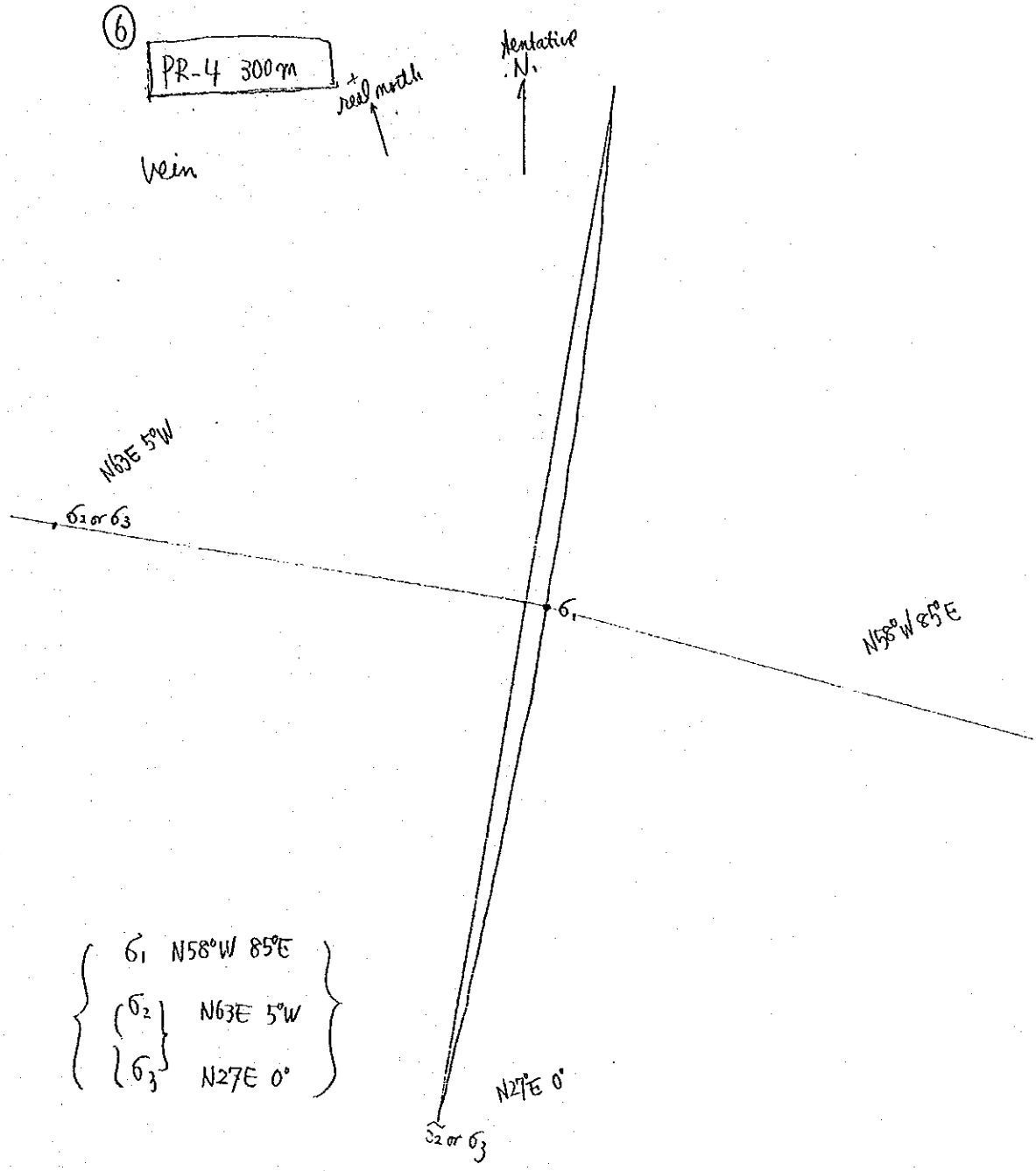

$$\left\{ \begin{array}{ll} \sigma_1 & N58°W\ 85°E \\ \left\{ \begin{array}{l} \sigma_2 \\ \sigma_3 \end{array} \right. & N63E\ 5°W \\ & N27E\ 0° \end{array} \right\}$$

⑦

PR-5

350m

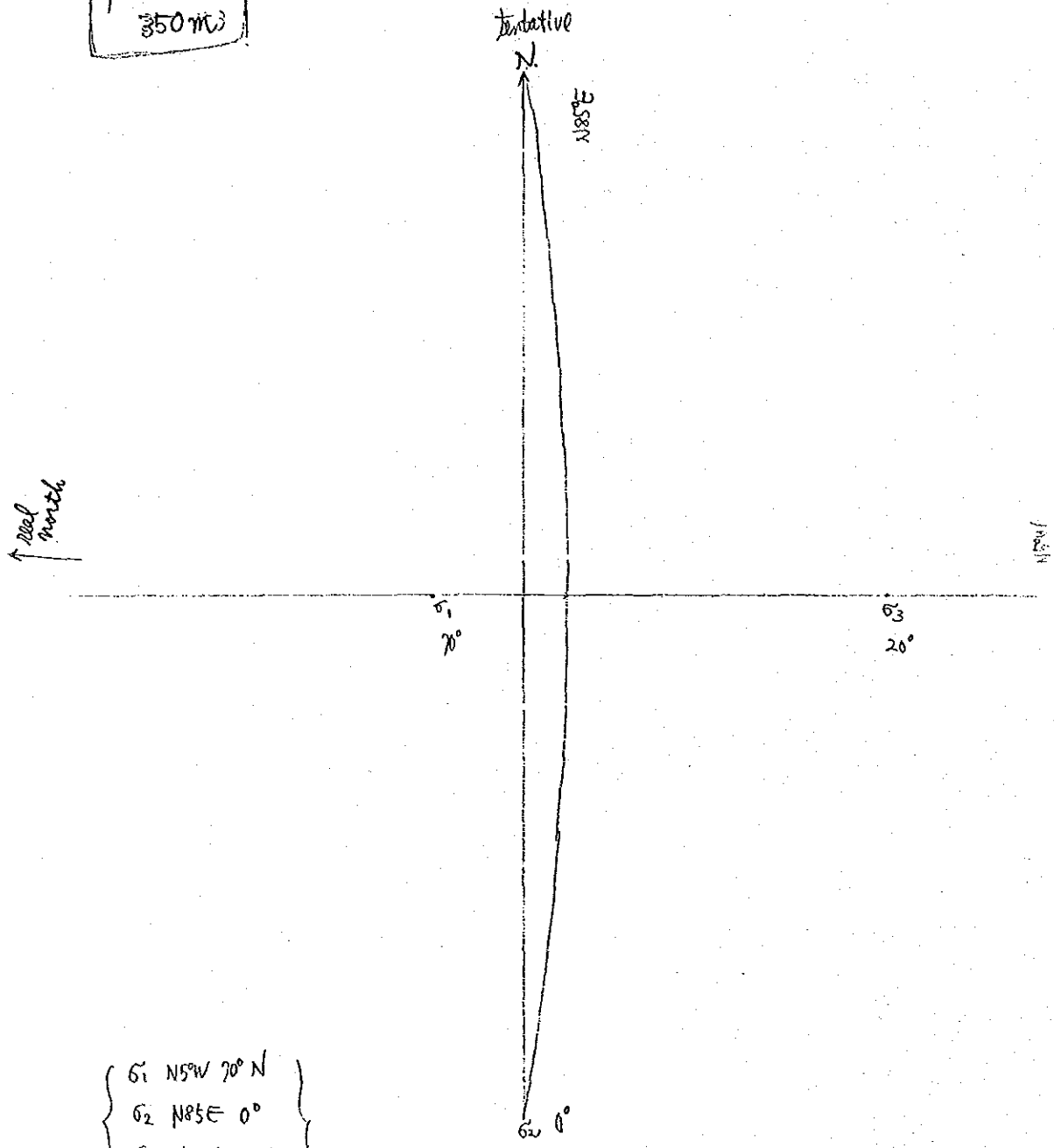

σ1 N5°W 70° N
σ2 N85E 0°
σ3 N5°W 20° S

⑧

RC-1 700m

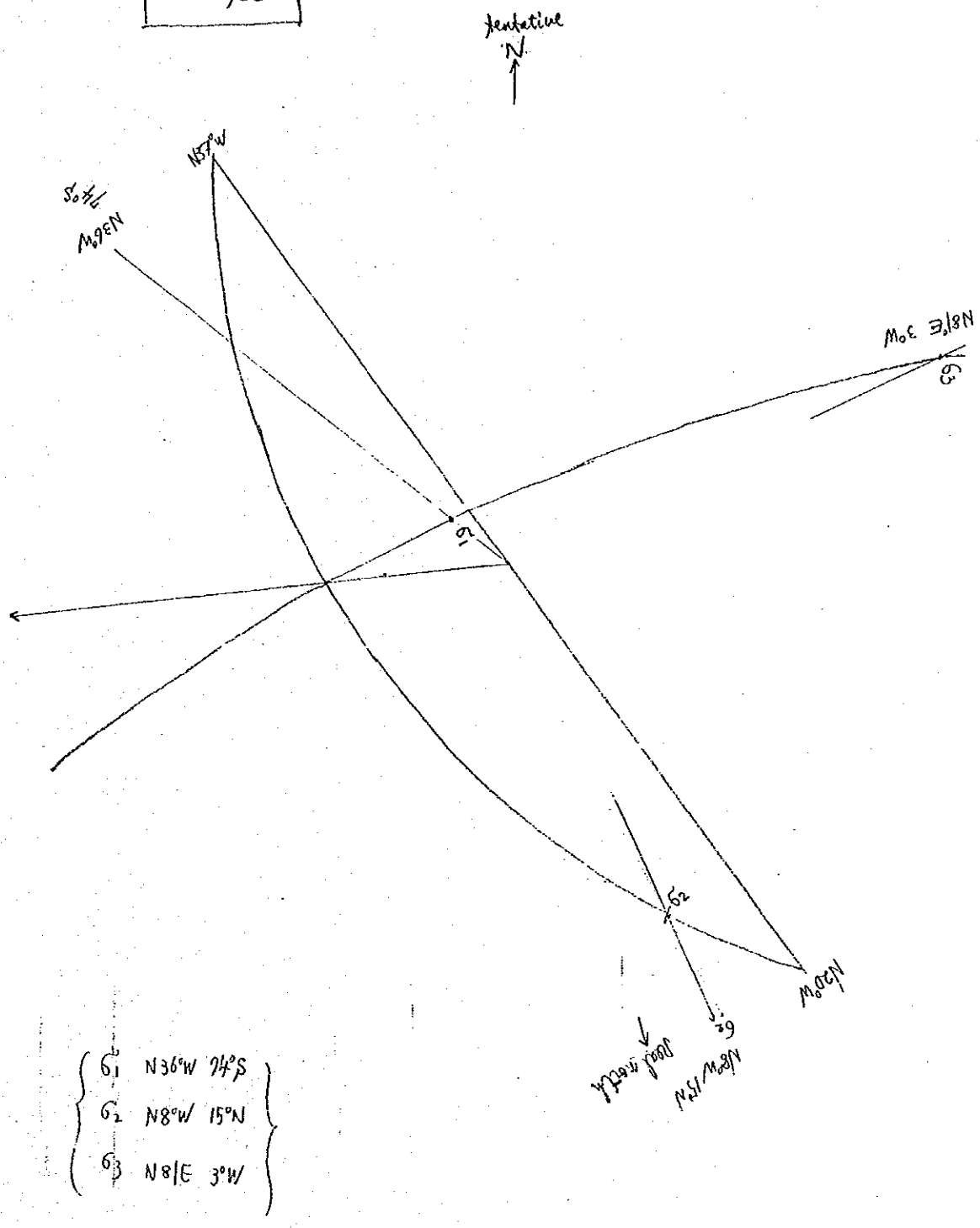

θ_1 N36°W 24°S

θ_2 N8°W 15°N

θ_3 N8|E 3°W